Second Annual Report
National Aeronautics and Space Administration
Langley Research Center
Grant NGR 23-004-091

THE VORCOM

Part 1: Analytical Considerations

Prepared by

John F. Foss

Division of Engineering Research
MICHIGAN STATE UNIVERSITY
East Lansing, Michigan 48824

Second Annual Report
National Aeronautics and Space Administration
Langley Research Center
Grant NGR 23-004-091

THE VORCOM
Part 1: Analytical Considerations

Prepared by
John F. Foss

Division of Engineering Research
MICHIGAN STATE UNIVERSITY
East Lansing, Michigan 48824
April 30, 1976

TABLE OF CONTENTS

Page

ABSTRACT

1. INTRODUCTION 1

2. COMPUTATION ALGORITHM FOR u, w GIVEN E_1, E_2 . . 4

2. 1. Pitch Angle Response 4
2. 2. Solution for the Pitch Angle 5
2. 3. Characteristic Results 7

3. ACCURACY AND UNCERTAINTY 8

3. 1. Accuracy 10
3. 2. Uncertainty 12

3. 2. 1. Uncertainty in γ 13
3. 2. 2. Uncertainty in V, u, and w 14
3. 2. 3. Uncertainty in ω_y 16

3. 2. 3. 1. Uncertainty in $\partial w/\partial x$ 17
3. 2. 3. 2. Uncertainty in $\partial u/\partial z$ 22
3. 2. 3. 3. Statement of Uncertainty for ω_y 26

REFERENCES 27

FIGURES 1 - 8 . . . . . 28 - 47

TABLES 1 - 3 . . . . . 48 - 50

ABSTRACT

The analytical considerations which support the computation of (i) two components of the velocity vector from an x-array and (ii) the transverse vorticity from the x-array and an adjacent parallel wire pair are presented herein. The electronic circuit which will execute these computations at a 50 khz rate is also described. The factors limiting the accuracy of the measurements are identified and quantitative estimates are given for a typical x-probe. An extensive analysis of the factors which effect the output and which are unknown (or unknowable) during the measurement is presented. Quantitative estimates of these effects are developed in the form of an uncertainty analysis. Numerical values, calculated using the analytical structure of the response equations, are tabulated; other estimates which require special experiments are described.

1. INTRODUCTION

The vorticity, which is a measure of the fluid particles rotation rate about its centroid, is a continuous function in space defined by the operation

$$\underset{\sim}{\omega} = \nabla \times \underset{\sim}{V} \tag{1}$$

The operation of forming the spatial derivative implies that $\underset{\sim}{\omega}$ contains less information than the original velocity field, $\underset{\sim}{V}$. For example, the vorticity is the antisymmetric part of the second order tensor which represents the spatial derivative of the velocity fields, specifically

$$\frac{\partial u_i}{\partial x_j} = \underbrace{\frac{1}{2}\left(\frac{\partial u_i}{\partial x_j} + \frac{\partial u_j}{\partial x_i}\right)}_{A} + \underbrace{\frac{1}{2}\left(\frac{\partial u_i}{\partial x_j} - \frac{\partial u_j}{\partial x_i}\right)}_{B} \tag{2}$$

where A is the rate of strain tensor and B is the rate of rotation tensor. The loss of information is, however, often compensated by an enhanced understanding of the flow field when the vorticity, and its time dependent behavior, are used for diagnostic purposes. Some examples and reference to several general examinations of vorticity considerations are provided below.

Lighthill [1963] presents an excellent summary of vorticity fundamentals and their relationship to the factors of interest in fluid mechanical descriptions. Vorticity in turbulent flows is given considerable attention by Tennekes and Lumley [1972]. The highly instructive photographs of large vortical structures in a shear layer by Roshko and co-workers (see, e.g., Brown and Roshko [1974]) is but one reference which suggests that large scale vortical motions are of critical importance in the description of turbulent shear flows. Direct measurements of the vorticity which constitutes the elementary ingredient of the large structure is clearly desirable, especially as it might provide some direct experimental evidence in relationship to the recently advanced theoretical (and provocative) arguments of Moore and Saffman [1975]. Turbulent shear flows, which are not bounded by a solid surface, are bounded by a thin region termed the viscous super layer. The rationale for the existence of this layer and theoretical considerations for many of its properties are developed in a comprehensive study by Corrsin and Kistler [1955]. The final stages of

entrainment of ambient flow into the shear flow is known to occur at this boundary; the relative importance and a description of the behavior of engulfment or the convective action of the pressure field associated with the corrugations of this interface would clearly be aided by an ability to execute detailed vorticity measurements in such flows. The characteristics of many technologically interesting flows can be modelled in terms of the behavior of their mean vorticity, see e.g., Foss and Kleis [1976]. The control volume form of the vorticity transport equations (Potter and Foss [1975], Chapter 5) shows the importance of the surface pressure gradient for such flows. The role of the time-dependent vorticity field in the production of acoustic noise has been developed in Eulerian form by Hardin [1973]. This relationship expresses the far field density fluctuation $\rho_a(\underset{\sim}{x}, t)$ as a function of the vorticity and velocity of the flow field; specifically

$$\rho_a(\underset{\sim}{x}, t) \approx \frac{-\rho_o}{4\pi a_o^4} \frac{x_i x_j}{x^3} \left(\frac{d^2}{dt^2} \int_V y_i \, _j \vec{d}y \right)^* + \frac{1}{4\pi a_o^4} \left|\frac{1}{x}\right| \frac{d^2 e}{dt^2} \qquad (3)$$

It is this last application which has been the principal motivation for the development of a capability to measure one component of the three-dimensional vorticity field; however, such a capability will also serve many other problem areas including those previously identified in this introductory section.

Comprehensive and careful measurements of the mean velocity field would allow the mean vorticity field to be evaluated; this however would not meet the desired capability! An instantaneous evaluation is required if a quantity such as $\partial^2(\underset{\sim}{\omega} \times \underset{\sim}{V})/\partial t^2$ is to be determined.

Consider a flow in which the gradient of the mean shear lies in the x-z plane. The transverse, or y-component, of vorticity is

$$\omega_y = \frac{\partial u}{\partial z} - \frac{\partial w}{\partial x}$$

The measurement of this component is the object of our effort. It has been selected because it represents the principal component in the class

of flows under consideration (the mean values of ω_x and ω_z are zero). In particular, it is important in the construction of $\underset{\sim}{\omega} \times \underset{\sim}{V}$ for the flow field of particular interest, viz., the normal impingement of an axisymmetric jet. It is shown in the following that this quantity can, in principle, be measured if one is willing to accept the approximation to a point measurement afforded by an array of probes and if one is willing to make further assumptions regarding the construction of the derivatives. The same probe configuration could be used to attempt a measurement of ω_z, albeit the approximations will be more severely tested by the presence of mean velocity gradients. The measurement of ω_x is much more involved in principle; however, a generally successful approximate technique is available; see Kistler [1952] or the report by Corrsin and Kistler [1955].

The essential strategy of the present measurement is demonstrated in the schematic representation of the vorticity probe shown in Figure 1. The quantity ω_y will be evaluated by the following procedure: (1) evaluate $|V|$ and γ as the two unknowns which are related to E_1 and E_2 of the x-wire probe; (2) construct $\partial w/\partial t$ for the time $(t+\Delta t)$ from the time series $w(t)$ as

$$\frac{\partial w}{\partial t}(t+\Delta t) = \frac{w(t+2\Delta t) - w(t)}{2\,\Delta t} \quad ;$$

(3) construct $\partial w/\partial x$ (at $t+\Delta t$) by utilizing the "frozen flow assumption

$$\frac{\partial w}{\partial x} \approx -\frac{1}{u}\,\frac{\partial w}{\partial t} \quad .$$

(4) construct $(\partial u/\partial z)$ from the readings of the parallel wires as

$$\frac{\partial u}{\partial z}(x, y, z) \cong \cos\gamma(x, y, z)\,\{[V(x, y+\Delta y,\ z+\Delta z) - V(x, y+\Delta y,\ z-\Delta z]/2\Delta z]\}$$

where the approximations resulting from the lateral displacement of the probe and the utilization of a single value of $\cos\gamma$ are immediately obvious.

The strategy of the measurement can be used to identify the specific considerations which represent the contributions of this report. First, a scheme to reliably compute $|V|$ and γ from E_1 and E_2 must be developed. This scheme is the subject of Section 2. The operation of forming the difference $[(\partial u/\partial z) - (\partial w/\partial x)]$ of two quantities which are

themselves differences suggests that questions of (1) accuracy and (2) uncertainty are of paramount importance in this study. If ω_y is to have integrity, or at least if the reliability of the final value is to be estimated, then considerable attention must be given to matters of accuracy and especially uncertainty. Section 3 presents a comprehensive evaluation of these matters.

It should be noted that the preliminary considerations of the response equations and the uncertainty estimates, as given by the present author in the Second Semi-Annual Report (Foss [1975]), are obviated by the developments reported herein. Specifically, an improved scheme to convert (E_1, E_2) into $(|V|, \gamma)$ has been developed and a considerably improved methodology for constructing the uncertainty considerations has been evolved. The earlier efforts were useful in the evolutionary process but they have been uniformly superseded by the present work.

2. COMPUTATION ALGORITHM FOR u, w GIVEN E_1, E_2

The response of an individual hot-wire channel is dependent upon the magnitude and direction of the velocity vector with respect to the hot-wire itself. If the yaw angle is zero (that is, if the cross-product between the velocity and a vector parallel to the wire is perpendicular to the probe axis), then the response of the two wires constitutes two equations for two unknowns. It is the purpose of this section to develop the algorithms by which the hardware of the VORCOM or software in a general purpose computer can be utilized to extract the magnitude and direction of the velocity vector given the two voltage readings.

2.1. Pitch Angle Response

Several pitch angle response equations have been offered in the general literature. A summary of the more prominent ones include:

Hinze [1959] and Champagne et al. [1967]

$$V_{eff} = |V|[\cos^2 \alpha + k^2 \sin^2 \alpha]^{1/2} \tag{8}$$

Fujita and Kovasznay [1968]

$$V_{eff} = |V|[\cos \alpha + \epsilon(\cos \alpha - \cos 2\alpha)] \tag{9}$$

Brunn [1971]

$$V_{eff} = |V| \cos^{m} \alpha \tag{10}$$

Friehe and Schwarz [1968]

$$V_{eff} = |V| \{1 - b[1 - \cos^{1/2} \alpha]\}^{2} \tag{11}$$

where α is the angle between the normal to the wire and the velocity vector. Note that each of these is based upon a modification of the "cosine law" which would be valid for a wire of infinite aspect ratio.

For the purposes of the present study, it was considered satisfactory to identify an effective pitch angle response formulation which fit the empirical data and was readily integrated into our computation scheme; the Friehe and Schwarz relationship was selected in response to these criteria.

2.2. Solution for the Pitch Angle

The computational strategy to recover α given E_1 and E_2 will be established in this section. The pertinent terms of the equations will first be defined.

A two-step data acquisition process will be utilized. The probe will first be aligned with the time mean flow; a time series of u, w, and ω_y will then be obtained. For an axisymmetric flow, the probe will be positioned in the x-r plane. The instantaneous velocity for the time series data will be described in terms of its pitch angle (γ) with respect to the probe. (The final data will, of course, be referenced to the x, r, θ laboratory coordinates.) Consequently, as shown in Figure 2, the pitch angles with respect to the hot-wires of the "x" array can be expressed as

$$\alpha_1 = \beta_1 - \gamma \quad \text{and} \quad \alpha_2 = \beta_2 + \gamma \tag{12}$$

where the β values are defined on the figure. The effective velocities are related to the hot-wire voltage values by the relationship

$$E_j^2 = E_{o_j}^2 + K_j(\alpha)\ V_{eff}^{mj} \qquad j = 1, 2 \tag{13}$$

where E_{o_j} and K are constants for a given overheat ratio and ambient temperature. A large number of calibration data sets generated in our laboratory have supported the original proposal of Collis and Williams [1959] that m = 0.45; however, the most appropriate value of the constant m is determined for each data set by the calibration process described elsewhere in this report.

The essence of the computational strategy is to compute γ from the voltage pair (E_1, E_2) and equations (11), (12), and (13). An explicit form for the relationship between E_1, E_2 and γ can be developed as

$$\frac{(E_1^2 - E_{o_1}^2)^{1/m_1}}{(E_2^2 - E_{o_2}^2)^{1/m_2}} = \frac{K_1^{1/m_1}}{K_2^{1/m_2}} \left\{ \frac{\{1-b_1[1-\cos^{1/2}(\beta_1-\gamma)]\}}{\{1-b_2[1-\cos^{1/2}(\beta_2-\gamma)]\}} \right\}^2 \qquad (14)$$

by using (11) in (13) and cancelling $|V|$.

The left side of (14) will be referred to as G_{meas} and the right side as <G> indicating that the right side is computed from the results of the prior averaging processes which yield $K(\gamma)$. It should be noted that $b_1 = b_2 = 0.92$ is assumed on the basis of the Friehe and Schwarz data and that $m_1 = m_2 = 0.45$ will be used unless a particular probe calibration appears to require different values. β_1 and β_2 will be individually evaluated from the symmetry point of the hot-wire angular response curves.

The magnitude of the velocity can be determined once the pitch angle is evaluated. Specifically

$$|V| = [E_1^2 - E_{o_1}^2]^{1/m} * F(\gamma) \qquad (15)$$

where $F(\gamma)$ is defined as

$$F(\gamma) = K(\gamma)^{-1/m} \{1-b[-\cos^{1/2}(\beta-\gamma)]\}^{-2} \qquad (16)$$

If the G_{meas} value was everywhere equal to the <G> value, then the above considerations would be sufficient for the calculation of γ and $|V|$. However, the calibration of $E_1(|V|, \gamma)$ and $E_2(|V|, \gamma)$ require the definition of the following quantity

$$G_{meas} - \langle G \rangle = A(\gamma) + S(\gamma)\,(|V| - \langle V \rangle) \qquad (17)$$

where the reference velocity of $\langle V \rangle$ is arbitrarily chosen as an approximate center point of the calibration data set. An iterative scheme for the assessment of the γ value is therefore suggested. The details of this computation and the calculation steps to be executed by the VORCOM are shown in Figure 3b. The schematic diagram showing the steps in the computation process is considered to be self-explanatory; the ability of a single iterative loop to evaluate the correct γ is discussed in the following section.

2.3. Characteristic Results

Several complete data sets have been obtained: $E_1(|V|,\gamma)$, $E_2(|V|,\gamma)$, for $10 \leq |V| \leq 120$ where

$$|V|_{i+1} = |V|_i \tilde{+} 10 \text{ fps}$$

and for $-40 \leq \gamma \leq 40$ degrees where $\gamma_{i+1} = \gamma_i + 5$ degrees are representative of the data base required for a complete set. These numbers have been used to establish the validity of the basic form of the response equation (including the determination of E_o) and to evaluate the functional form for $K(\gamma)$ from which the following are obtained:

$$\langle G(\gamma) \rangle, \quad F(\gamma), \quad S(\gamma), \quad A(\gamma) .$$

Graphical representations of these relationships are presented in Figures 4 through 6 and Table 1. The $A(\gamma)$ and $S(\gamma)$ values of Table 1 suggest that these quantities are not a smooth function of γ. This lack of smoothness is attributed to their small numerical values and hence to their susceptibility to inaccuracies; however, this is not deemed to represent a significant degradation in their utility for the calculation scheme. Table 1 also includes the standard deviation (S.D.) of the quantity GDIFF where GDIFF $\equiv G_{meas} - \langle G \rangle$ and

$$\text{S.D.} = \frac{1}{(N-1)} \sum_{i=1}^{N} \{[\text{GDIFF}]_{i,\,\text{actual}} - A(\gamma) + S(\gamma)\,(V_i - 55)\}^2$$

(Note that $\langle V \rangle = 55$ fps is used for this data set.)

This standard deviation is, in some cases, a significant fraction of GDIFF itself; however, in all cases the quantity which represents the effect on the calculation of γ is small. Specifically, let γ_{error} represent the error resulting from the use of a linear approximation of GDIFF, then

$$\gamma_{error} = \frac{d\gamma}{dG} \text{ S.D.}$$

The values of γ_{error} are also presented in Table 1; these small values justify the adoption of the indicated calculation procedures.

The G_{meas} values are identified in Figure 5 for the set of velocities $10 \leq |V| \leq 120$ fps. From this presentation, it is apparent that G_{meas} is quite close to $<G>$ for the small absolute values of γ and that the deviations between G_{meas} and $<G>$ are small but not a smooth function of γ. The linear form used in (17) was selected for computational convenience and because of the monotonic dependence of the difference in the G values with respect to V. The pertinent feature is the ability to recover the correct γ value from the E_1 and E_2 values. An evaluation of this "recovery ability" is included in the discussion of "accuracy," see Section 3.1.

The ability to recover $|V|$ given γ is a more precise process. The validity of the $K(\gamma)$ evaluation from the initial calibration data sets is felt to be essentially limited by the accuracy of the V calculation based upon the measured total pressure. Since K is a smooth function of γ and since the resulting $F(\gamma)$ is also smooth, there seems little additional uncertainty in these calculations once γ is known. This assertion is also evaluated in Section 3.1.

3. ACCURACY AND UNCERTAINTY

The central question to be addressed by this section is:

> Given E_1, E_2, E_3, E_4 as voltages from the hot-wire channels and given the calibration data and computational procedures described in the previous section, what is the relationship between the calculated u, w, and ω_y values and the values of the same quantities which exist in the jet flow.

The response to this question is best constructed in terms of the accuracy and the uncertainty of the measures. It is useful to first provide

an explicit definition of the two words. *

accuracy: degree of conformity of a measure to a standard or true value

uncertainty: not having certain knowledge

We will here speak of the accuracy of the computation of u, w, ω_y given E_1, E_2, E_3 and E_4 for "known" conditions of the flow field as the "accuracy of the computing procedures." There are three aspects to the designation of the accuracy. First, the calibration data, which are used to compute E_o^2, $K(\gamma)$ and β, are known at discrete values of the velocity and the pitch angle γ; hence, it is necessary to construct interpolation schemes for the construction of intermediate values. Second, the control variable V is not precisely known during the calibration process; that is, the total pressure required for the calculation of V is limited by the available accuracy of the capacitive pressure transducer. Third, the accuracy of the hot-wire voltage reading is limited by the A/D converter resolution; specifically, the voltage span of $0 \leq E \lesssim 4$ volts will be processed by the 12 bit A/D converted of the Texas Instruments minicomputer (in the calibration process) and the approximately 1-1.2 volt active portion of the signal ($E_o \leq E \leq E_{max}$) will be processed by a high speed (4 μsec) 10 bit A/D converter for the data acquisition. In both situations, the expected resolution is of the order 1-1.5 mv. Significantly, the noise of the hot-wire anemometer is $\lesssim$ 1.5 mv; hence, noise will only effect the least significant bit of the reading. It should be noted that this noise level includes the beneficial effect of the 20 μsec averaging time; this is essentially a low pass filtering operation and, as such, it removes the high frequency noise of the anemometer circuitry. Spurious effects such as d.c. drift of the amplifiers, changes in the ambient temperature level and dirt accumulation on the probes will be limited by careful monitoring of the experiment. The specific aspects of the accuracy of the computing process are evluated in subsection 3.1.

When the four-wire probe is located in the jet flow, the factors which result in the observed voltages cannot be uniquely identified in

*Websters New Collegiate Dictionary

terms of the values V and γ. That is, a transverse velocity component v may be present in addition to the u and w components in the plane of the x-wire. Secondly, the possibility of a gradient in the pitch angle γ and/or the velocity magnitude V must be recognized. These effects cannot be ascertained using the signals of the x-wire array. However, the effects of these additional factors can be analytically modeled and their magnitudes can be represented by appropriate statistical measures. Because the instantaneous values, which will comprise the time series for u, w, and ω_y, are influenced by effects which are unknown, i.e. by factors which are represented by our "... not having certain knowledge ...," we refer to these effects as representing an uncertainty in the values for u, w, and ω_y. These considerations are discussed in full in subsection 3.2.

3.1. Accuracy

A sequence of operations is required to assess the velocity in the flow field. The essential feature which defines the accuracy of this process is the identification of the least accurate step in the sequence. The three major steps in the sequence are identified in the opening discussion of Section 3; they are (1) reliability of the interpolation formulae, (2) measurement of velocity in the calibration process, (3) A/D converter resolution and the noise level of the hot-wire anemometer.

The measurement of the velocity in the calibration process is considered to be the limiting factor in the accuracy of the measurements to be made with the VORCOM. Specifically, the linearity specification for the capacitive pressure transducer and the nonlinear $V \sim \sqrt{p}$ relationship results in a nearly constant 0.5 fps resolution in the velocity. This a priori assessment has been indirectly verified by numerous calibrations of various wires and the subsequent calculations of the standard deviation of $[V_{HWA} - V_{meas}]$. A typical set of calibration data is reproduced in Table 2 and is presented graphically in Figure 7.

The accuracy of the interpolation relationships described in Section 2 is difficult to assess given the recognized accuracy limits of the original velocity measurements. However, it has been found that the functional form

$$E^2 = E_o^2 + K V_{eff}^m \qquad (18)$$

fits the calibration data to within a nominal value (standard deviation) of $\simeq 0.6$ fps if a constant value of m is used for the fit; see Table 2. The calibration data invite the following rather interesting speculative considerations regarding the recoverable accuracy of velocity measurements. Specifically, if the above relationship (18) is accepted as valid, and if the hot-wire voltage measurement is accurate (to within the noise limitation of the instrument) then the hot-wire voltage can provide velocity measurements with an accuracy exceeding that of the original calibration. That is, the standard deviation quoted above reflects the uncertainty in the velocity as monitored by the pressure transducer, a more accurate measurement of V_{meas} would conform to the V_{HWA} as deduced from the E_o and K values of the calibration process.*

The precision of the 10 bit A/D converter and table-look-up operation of the VORCOM is decidedly not the limiting factor in the sequence of operations. Specifically, the conversion/look-up process can provide $\simeq 0.1$ percent resolution over the full range of values; the accuracy of the measurement is given by the estimated $\pm$ 0.5 fps ambiguity in the calibration velocities which corresponds to $\pm$ 5 percent accuracy at 10 fps and $\pm \approx 0.5$ percent accuracy at 120 fps. Hence, the accuracy of the measurement is limited by the accuracy of the original velocity measurement and not by the resolution of the signal processing equipment.

Since these estimates of the accuracy are based upon a number of assumptions, it is useful to also characterize the accuracy for a given data set in terms of the ability to recover the known $|V|$ and (γ). This comparison is presented in Table 3. The calculated values are derived from the E_1 and E_2 values of the calibration data set; they are respectively compared with the γ, which was set in the calibration process, and the V, which was calculated from the pressure transducer. As noted above, Section 3.1, deviations up to $\pm$ 0.5 fps can be expected as a result of the pressure transducer characteristics. The comparison between $|V|_{calc}$ and $|V|_{meas}$ and that between γ_{calc} and γ_{meas} are presented as both a percentage and as an absolute value for each velocity, pitch angle pair.

*Brunn [1971] makes use of calibration data over the range $0.4 \leq V \leq 150$ mps to evaluate m(V). In the range of current interest $3 \lesssim V \lesssim 40$ mps, a a constant value of m is also supported by his data.

The accuracy level implied by the ± 0.5 fps estimate is quite adequate for the determination of the velocity magnitude. As will be evident in the following section, the inescapable uncertainties associated with the measurement of u, w, and ω_y in the hostile environment of a turbulent flow will be the limiting factor in the interpretation of the original data. In this regard, it is especially important to note that the differencing operations of the voriticity evaluation are sensitive to whether the accuracy limitation results from erratic or smooth perturbing effects. The nonlinearity of the pressure transducer and the inaccuracies of the interpolation formulae are all "smooth" in character. Hence, the contribution of the inaccuracy will tend to cancel out with the differencing operation. Electronic noise would, of course, be erratic and would make a statistically significant contribution were it not for its small magnitude ($\simeq 0.1$ percent of the voltage measurement).

3.2. Uncertainty

The factors influencing the uncertainty will be traced by following the signal processing sequence to yield the u, w, and ω_y values (referenced to the probe coordinates). The following convention is introduced for this analysis:

i. The measured value of the quantity of interest, [ ], will be expressed as its "true" value, $[\ ]_T$, plus a difference term, $\delta[\ ]$.

$$[\ ] = [\ ]_T + \delta[\ ] \tag{19}$$

ii. The relative value of the difference term is expressed as $\epsilon_{[\ ]}$ and is defined by the expression

$$\epsilon_{[\ ]} = [\ ]/[\ ]_T - 1 . \tag{20}$$

In the context of this discussion, the "true" value, $[\ ]_T$, will not include the considerations of accuracy as presented in Section 3.1. That is, we seek only to describe the effects of the actual flow field which result in our "not having certain knowledge" as regards the relationship of the measured to the true value of the quantity [ ].

The meaning of the uncertainty can be further defined by noting that (i) the uncertainty of the calibration data is zero and (ii) the causal factors of the uncertainty are known but their magnitude and hence their influence on each individual reading are both unknown and, for the experimental capability at hand, unknowable.

The strategy for the evaluation of the uncertainties follows from the second condition; namely, the (unknowable) effects in the flow field which influence the magnitude of the measured quantity [ ] will be analytically incorporated into the calculation formulae for [ ]. The magnitude of the disturbing effect will then be characterized by its standard deviation to allow the value of $\epsilon_{[\ ]}$ to be evaluated. The final results will be presented as ϵ_γ, ϵ_u, ϵ_w and $\epsilon'_{\partial/\partial x}$ where the $\epsilon_{[\ ]}$ values are functions of γ and are parametrically dependent upon the quantities $\Delta\gamma$, $\Delta V/V$ and v/V which are defined below. The ϵ_{ω_y} values are dependent upon the results of special experiments to be executed; however, estimates of that fraction of the ϵ_{ω_y} values that can be extracted from these purely analytical considerations are also presented in the following.

The perturbing effects, which create the uncertainties, are a result of the three-dimensional, spatially nonuniform conditions of the actual (turbulent) flow fields. Specifically, the magnitude of the velocity, $|V|$, and the pitch angle, γ, may be different at the two wires of the x-probe. In addition, it can be expected that a lateral velocity, v, will be present in the flow and hence $|V| = [u^2 + w^2 + v^2]^{1/2}$ as compared with the calibration condition in which $|V| = [u^2 + w^2]^{1/2}$.

These three effects will be characterized by the quantities $(\Delta V/V)$, $\Delta\gamma$, and (v/V) where the Δ quantities are the difference values between the two wires.

3.2.1. Uncertainty in γ

The pitch angle γ is determined from the magnitude of the G function. The uncertainty in γ can be determined by evaluating the effect of the three perturbation quantities, $\Delta\gamma$, $(\Delta V/V)$ and (v/V), on the magnitude of G and hence on the magnitude of γ. The latter relationship can be expressed as $\delta\gamma$ (where $\delta\gamma \equiv \gamma_T - \gamma$)

$$\delta\gamma = \frac{d\gamma}{dG}\,\delta G \tag{21}$$

and

$$\delta G = G - G_T \tag{22}$$

The quantity G represents the value obtained by the computation procedure described in Section 2; that is, $G_{meas} \rightarrow \gamma_1 \rightarrow F(\gamma_1) \rightarrow |V| \rightarrow [G_{meas} - \langle G \rangle] \rightarrow \langle G(\gamma_2) \rangle \rightarrow \gamma_2$ and $\langle G(\gamma_2) \rangle$ is the G value of equation (22).* The true value of G (i.e., G_T) is (defined to be) that value which would have been produced by the same steps if $\Delta\gamma$, $(\Delta V/V)$ and (v/V) were identically zero. Since an explicit relationship for G is available, the quantity δG can be computed as

$$\delta G\,[\gamma, |V|; \Delta\gamma, (\Delta V/V), (v/V)] = G[\gamma, |V|; \Delta\gamma, \Delta V/V, v/V] - G[\gamma, |V|] \tag{23}$$

where

$$G[\gamma, |V|; \Delta\gamma, (\Delta V/V), (v/V)] = \frac{K_1(\gamma_1)^{1/m_1}[\{1-b[1-\cos^{1/2}(\beta_1-\gamma_1)]\}^4 + (v/V)^2]^{1/2}\,V_1}{K_2(\gamma_1+\Delta\gamma)^{1/m_2}[\{1-b[1-\cos^{1/2}(\beta_2-\gamma_1-\Delta\gamma)]\}^4 + \{v_1+\Delta v/(V_1+\Delta V)\}^2]^{1/2}(V_1+\Delta V)} \tag{24}$$

An immediate simplification appears to be in order, viz., $\Delta v = 0$ will be assumed.

The desired quantity, $\delta\gamma$, follows from equations (21), (22), (23), and (24) where $G[\gamma, |V|]$ is obtained by setting $\Delta\gamma = \Delta V = v = 0$ in (24) and where the explicit dependence upon V can be eliminated as seen by (24).

3.2.2. Uncertainty in V, u, and w

The calculation of V requires a known value for γ and the voltage E_1. The computing equation is based upon the assumption that the velocity is in the x-z plane; that is, that the conditions of the calibration process

*Note that the subscripts 1 and 2 refer to the initial and first iteration values for γ; see Figure 3b. However, the subscripts in (24) refer to wire 1 and wire 2 of the x-array.

are duplicated in the flow field. Hence v exerts an implicit ($\delta\gamma = \delta\gamma(v/V, \ldots)$) and an explicit perturbing effect on the $|V|$ uncertainty. The development of ϵ_V can be constructed by approximating V_T with the expression

$$E_1^2 = E_{o_1}^2 + K_1(\gamma_T)[\{1-b[1-\cos^{1/2}(\beta_1-\gamma_T)]\}^4 + (v/V_T)^2]^{m/2}|V_T|^m \tag{25}$$

which presumes that the response equation (18) is unequivocally valid and that γ_T is the pitch angle at wire 1. The unequivocal valididty of (18) implies that the pitch angle relationship, including the value of K, is not effected by the presence of a non-zero yaw angle. Hence V_T of (25) is the velocity magnitude in the plane of the x-wire, viz. $|V_T| = (u_T^2 + w_T^2)^{1/2}$.

The value of $|V|$ which is determined by the computing equations is based upon the measured E_1, the spurious γ (i.e., $\gamma_T + \delta\gamma$) and the neglect of the lateral velocity v. This value can also be expressed using equation (18), viz.,

$$E_1^2 = E_{o_1}^2 + K(\gamma_T+\delta\gamma)\{1-b[1-\cos^{1/2}(\beta_1-\gamma-\delta\gamma)]\}^{2m}|V|^m \tag{26}$$

By subtracting E_o^2 from both sides and making use of the definition of $\epsilon_{[\ ]}$, see (19), the quantity ϵ_V can be expressed as $\epsilon_V = V/V_T - 1$, hence

$$1+\epsilon_V = \left[\frac{K(\gamma_T)}{K(\gamma_T+\delta\gamma)}\right]^{1/m_1} \frac{[\{1-b[1-\cos^{1/2}(\beta_1-\gamma_T)]\}^4 + (v/V_T)^2]^{1/2}}{\{1-b[1-\cos^{1/2}(\beta_1-\gamma_T-\delta\gamma)]\}^2} \tag{27}$$

The uncertainty estimates for u and w follow from the ϵ_V and $\delta\gamma$ values which have been established above. The expressions for ϵ_u and ϵ_w are based upon the definitions for u and w, viz.,

$$u = V\cos\gamma \quad \text{and} \quad w = V\sin\gamma \tag{28}$$

Substituting $u_T + \delta u$ for u, $V_T + \delta V$ for V and $\gamma_T + \delta\gamma$ for γ, yields

$$u_T + \delta u = (V_T + \delta V)\cos(\gamma_T + \delta\gamma)$$

$$= (V_T + \delta V)(\cos\gamma_T \cos\delta\gamma - \sin\gamma_T \sin\delta\gamma)$$

$$\cong V_T \cos\gamma_T - V_T\delta\gamma \sin\gamma_T + \delta V \cos\gamma_T - \delta V\, \delta\gamma \sin\gamma_T$$

$$= V_T \cos\gamma_T [1 - \delta\gamma \tan\gamma_T + \epsilon_V - \epsilon_V \delta\gamma \tan\gamma_T]$$

or

$$\epsilon_u = [\epsilon_V - \delta\gamma \tan\gamma_T - \epsilon_V \delta\gamma \tan\gamma_T] \tag{29}$$

Similarly,

$$w_T + \delta w = (V + \delta V)\sin(\gamma_T + \delta\gamma)$$

$$= (V + \delta V)[\sin\gamma_T \cos\delta\gamma + \cos\gamma_T \sin\delta\gamma]$$

$$= V \sin\gamma_T + V\,\delta\gamma \cos\gamma_T + \delta V \sin\gamma_T + \delta V\,\delta\gamma \cos\gamma_T$$

$$= V \sin\gamma_T [1 + \delta\gamma \cot\gamma_T + \epsilon_V + \epsilon_V\, \delta\gamma \cot\gamma_T]$$

or

$$\epsilon_w = [\delta\gamma \cot\gamma_T + \epsilon_V + \epsilon_V\, \delta\gamma \cot\gamma_T] \tag{30}$$

Representative conditions for $(\Delta V/V)$, $\Delta\gamma$, and $(\Delta v/V)$ have been used to compute numerical values of the uncertainties $\delta\gamma$, ϵ_u, and ϵ_w. The results of these calculations are summarized in Figure 8.

3.2.3. Uncertainty in ω_y

The vorticity component transverse to the time mean streamline (and hence to the probe axis), ω_y, is defined as

$$\omega_y = \frac{\partial u}{\partial z} - \frac{\partial w}{\partial x}$$

The y component vorticity is constructed as the difference of two quantities which are themselves differences; numerous factors must be considered in its evaluation.

The uncertainty, $\delta\omega_y$, is defined by the expression

$$\omega_y = \omega_y]_T + \delta\omega_y \tag{31}$$

Since the uncertainty can also be expressed as a Taylor expression about the true value $\omega_y]_T$, the form

$$\omega_y = \omega_y]_T + \frac{\partial \omega_y}{\partial(\partial u/\partial z)} \left(\frac{\partial u}{\partial z}\right) + \frac{\partial \omega_y}{\partial(\partial w/\partial x)} \delta \left(\frac{\partial w}{\partial x}\right) + \ldots \qquad (32)$$

is appropriate. Hence,

$$\delta\omega_y = \delta(\partial u/\partial z) - \delta(\partial w/\partial x) \qquad (33)$$

if the linearization of the Taylor series is valid, that is, if $\delta(\partial u/\partial z)$ and $\delta[\partial w/\partial x]$ are sufficiently small. Such a condition will be assumed. It will be convenient to further subdivide this subsection in order to allow separate considerations of the uncertainty in $\partial w/\partial x$ and $\partial u/\partial z$.

3.2.3.1. Uncertainty in $\partial w/\partial x$

The quantity $\partial w/\partial x$ can be formed from the instantaneous z-component Navier-Stokes equations. Specifically,

$$\left.\frac{\partial w}{\partial x}\right]_T = -\frac{1}{u}\left[\frac{\partial w}{\partial t} + v\frac{\partial w}{\partial y} + w\frac{\partial w}{\partial z} + \frac{1}{\rho}\frac{\partial p}{\partial z} - \nu\frac{\partial^2 w}{\partial x_j \partial x_j}\right] \qquad (34)$$

If the "frozen flow" assumption, which is implicit in the Taylor hypothesis, is made then the following formulation is a rational construction for $\partial w/\partial x$

$$\frac{\partial w}{\partial x} = -\frac{1}{u}\frac{\partial w}{\partial t} \qquad (35)$$

An expression for the uncertainty $\epsilon_{\partial/\partial x}$ will be extracted from (34) and (35); $\epsilon_{\partial/\partial x}$ is defined by the expression

$$\frac{\partial w}{\partial x} = \left.\frac{\partial w}{\partial x}\right]_T [1 + \epsilon_{\partial/\partial x}] \qquad (36)$$

Substituting (34) and (35) into (36) yields,

$$\frac{1}{u}\frac{\partial w}{\partial t} = \frac{1}{u}\left[\frac{\partial w}{\partial t} + v\frac{\partial w}{\partial y} + w\frac{\partial w}{\partial z} + \frac{1}{\rho}\frac{\partial p}{\partial z} - \nu\frac{\partial^2 w}{\partial x_j \partial x_j}\right][1 + \epsilon_{\partial/\partial x}]$$

or

$$1 = \left[1 + \frac{v \frac{\partial w}{\partial y} + w \frac{\partial w}{\partial z} + \frac{1}{\rho} \frac{\partial p}{\partial z} - \nu \frac{\partial^2 w}{\partial x_j \partial x_j}}{\frac{\partial w}{\partial t}} \right] [1 + \epsilon_{\partial/\partial x}] \qquad (37)$$

Considering that $\epsilon_{\partial/\partial x} << 1$, the following approximation for $\epsilon_{\partial/\partial x}$ can be derived

$$\epsilon_{\partial/\partial x} \cong - \{ v \frac{\partial w}{\partial y} + w \frac{\partial w}{\partial z} + \frac{1}{\rho} (\frac{\partial p}{\partial z}) - \nu \frac{\partial^2 w}{\partial x_j \partial x_j} \} / (\partial w / \partial t) \qquad (38)$$

The expression for $\partial w/\partial x$ shows that this quantity is also influenced by the uncertainties associated with u and w. Consequently, the uncertainty $\epsilon_{\partial w/\partial x}$ is defined by the expression

$$\frac{\partial w}{\partial x} = \frac{1}{u_T(1+\epsilon_u)} \frac{\partial w_T(1+\epsilon_w)}{\partial t} [1 + \epsilon_{\partial/\partial x}]. \qquad (39)$$

The quantity $\partial w_T(1+\epsilon_w)/\partial t$ can be operated upon to yield

$$\frac{\partial w_T(1+\epsilon_w)}{\partial t} = \frac{\partial w_T}{\partial t} \{ 1 + \epsilon_w + \frac{w_T}{\partial w_T/\partial t} (\frac{\partial \epsilon_w}{\partial t}) \} \qquad (40)$$

$$\frac{w_T}{(\frac{\partial w_T}{\partial t})} \frac{\partial \epsilon_w}{\partial t} = \frac{w_T}{(\frac{\partial w_T}{\partial t})} \frac{\partial (\delta_w / w_T)}{\partial t}$$

$$= \frac{w_T}{(\frac{\partial w_T}{\partial t})} [\frac{1}{w_T} \frac{\partial \delta w}{\partial t} - \frac{\delta w}{w_T^2} \frac{\partial w_T}{\partial t}]$$

$$= \frac{\frac{\partial \delta w}{\partial t}}{\frac{\partial w_T}{\partial t}} - \frac{\delta w}{w_T}$$

$$\cong (|\epsilon_w| - \epsilon_w) \qquad (41)$$

where the last step involves the central assumption that the ratio of the time derivatives is adequately represented by the ratio of the arguments

of the differentiated quantities, namely $\delta w/w_T \simeq |\epsilon_w|$. Therefore,

$$\frac{\partial w_T(1+\epsilon_w)}{\partial t} \cong \{1 + |\epsilon_w|\} \frac{\partial w_T}{\partial t} \tag{42}$$

and

$$\frac{\partial w}{\partial x}(1+\epsilon_{\partial w/\partial x}) = \frac{1}{u_T} \frac{\partial w_T}{\partial t} \{1 + |\epsilon_w| - \epsilon_u + \epsilon_{\partial/\partial x}\}$$

$$\cong \frac{1}{u_T} \frac{\partial w_T}{\partial t} \{1 + [\epsilon_w^2 + \epsilon_u^2 + \epsilon_{\partial/\partial x}^2]^{1/2}\} \tag{43}$$

It should be noted that $\epsilon_{\partial/\partial x}$ will have to be evaluated from supplementary experiments as described in the following.

The evaluation of the quantity $\epsilon_{\partial/\partial x}$ required the evaluation of spatial derivatives of velocity and pressure, see equation (38). For convenience, the spatial derivatives will be grouped into three quantities to be separately discussed; the groups are $(v\,\partial w/\partial y + w\,\partial w/\partial z)$, $\rho^{-1}\,\partial p/\partial z$, and $\nu\,\partial^2 w/\partial x_j\,\partial x_j$.

The magnitude of the kinematic viscosity times the sum of the second derivatives $(\nu\,\partial^2 w/\partial x_j\,\partial x_j)$ is expected to be small; specifically, it is expected that the second derivatives themselves are small. The y and z derivatives are not accessible,* the quantity $\partial^2 w/\partial x^2$ can be approximated using the same Taylor hypothesis which is presently under investigation. If it is assumed that the small scales of the motion which are responsible for $\partial^2 w/\partial x^2$ are essentially isotropic, then

$$\frac{\partial^2 w}{\partial x_j\,\partial x_j} \simeq (2\sqrt{2} + 1)\frac{\partial^2 w}{\partial x^2} = 3.83\,\frac{\partial^2 w}{\partial x^2} \tag{44}$$

and, from the frozen flow approximation,

*A total of six channels of anemometry and three x-wires would be required, i.e., $\partial^2 w/\partial y^2 \simeq [w(y+\Delta y) - w(y-\Delta y)]/2\Delta y$ would require two x-wires and four channels, $\partial^2 w/\partial z^2$ could be obtained from an additional x-wire at $(y, z+\Delta z)$.

$$\frac{\partial^2 w}{\partial x^2} \simeq 3.8 \left[\frac{1}{u^2} \frac{\partial^2 w}{\partial t^2} - \frac{1}{u^3} \frac{\partial w}{\partial t} \frac{\partial u}{\partial t} \right] \tag{45}$$

The mean square pressure gradient $\partial p/\partial z$ in isotropic turbulence has been analytically related to the longitudinal correlation function, see Hinze [1975], p. 308. Since the pressure gradient is sensitive to the small scales of the motion and since, as in the above assumption for $\partial^2 w/\partial x^2$, local isotropy is (perhaps) reasonable. We will make use of this relationship to estimate $\overline{(\partial p/\partial z)^2}$.

$$\overline{\left(\frac{\partial p}{\partial z}\right)^2} = \overline{\left(\frac{\partial p}{\partial x}\right)^2} = 4 \rho^2 u'^4 \int_0^\infty \frac{1}{r'} f(r')\, dr' \tag{46}$$

where u' is the r.m.s. value of the longitudinal velocity and f(r) is the longitudinal correlation function. By again invoking the frozen flow hypothesis for the construction of f(r), a time series for u(t) is sufficient to evaluate the mean square pressure gradient.

It is expected that the quantity $(v\, \partial w/\partial y + w\, \partial w/\partial z)$ may be quantitatively significant with respect to $\partial w/\partial t$; hence its magnitude must be assessed as accurately as possible. A complete measurement of this quantity by finite difference techniques is not feasible since three x-wire probes would be required for $v\, \partial w/\partial y$ alone and this measurement should be made simultaneously with $w\, \partial w/\partial z$ which would require two additional x-wire probes... 10 channels of anemometry and a "forest" of hot-wires. Consequently, the experimental evaluation of the desired quantity must necessarily involve rather substantial approximations. Several alternative schemes were considered; the following is deemed to represent the optimal evaluation of the quantity.

Consider that an x-probe is oriented to measure the z component velocity and that it is placed at $(x,\ y + \Delta y,\ z + \Delta z)$; this location will be referenced as $+\Delta$. A second x-probe is located at $(x,\ y - \Delta y,\ z - \Delta z)$; this location is term $-\Delta$. The z component velocity at $+\Delta$ is related to that at $-\Delta$ by the expression

$$w(+\Delta) = w(-\Delta) + \frac{\partial w}{\partial y} 2\Delta y + \frac{\partial w}{\partial z} 2\Delta z + \frac{\partial^2 w}{\partial y^2} \frac{(2\Delta y)^2}{2!} + \frac{\partial^2 w}{\partial z^2} \frac{(2\Delta z)^2}{2!} + \frac{\partial w}{\partial y \partial w} \Delta y \Delta z + \ldots \tag{47}$$

The quantity $\partial w/\partial y + \partial w/\partial z$ can be extracted as

$$\frac{\partial w}{\partial y} + \frac{\partial w}{\partial z} \cong \frac{w(+\Delta) - w(-\Delta)}{2\Delta z} + R \tag{48}$$

where $\Delta z = \Delta y$ is ensured by the placement of the probes and where the higher order terms R will be as sumed to be negligible. The assumption is rational if the probe displacement is sufficiently small. The desired quantity differs from that given in (48); viz.,

$$v\frac{\partial w}{\partial y} + w\frac{\partial w}{\partial z} \quad \text{versus} \quad \frac{\partial w}{\partial y} + \frac{\partial w}{\partial z}$$

The above epxerimental arrangement allows $w(x, y, z)$ to be approximated as

$$w(x, y, z) \simeq \frac{w(+\Delta) + w(-\Delta)}{2} \tag{49}$$

and, if the further assumption is made that $w \simeq v$, then

$$\begin{aligned} v\frac{\partial w}{\partial y} + w\frac{\partial w}{\partial z} &\simeq w(x, y, z)\left(\frac{\partial w}{\partial y} + \frac{\partial w}{\partial z}\right) \\ &\simeq \frac{w(+\Delta) + w(-\Delta)}{2}\left(\frac{w(+\Delta) - w(-\Delta)}{2\Delta z}\right) \\ &= \frac{w^2(+\Delta) - w^2(-\Delta)}{4\Delta z} \end{aligned} \tag{50}$$

The assumption that $v \simeq w$ is conservative since it is known that $\overline{vw} = 0$. Hence, the uncertainty $\epsilon_{\partial/\partial x}$ can be written as (see (43))

$$\begin{aligned} (\epsilon_{\partial/\partial x})^2 &= \left\{\left[v\frac{\partial w}{\partial y} + w\frac{\partial w}{\partial z}\right]^2 + \left[\nu\frac{\partial^2 w}{\partial x_j\,\partial x_j}\right]^2 + \left[\frac{1}{\rho}\frac{\partial p}{\partial z}\right]^2\right\} \Big/ \left(\frac{\partial w}{\partial t}\right)^2 \\ &= \left(\frac{\Delta t}{2\Delta z}\right)^2 \left[\frac{w^2(+\Delta) - w^2(-\Delta)}{w(t+\Delta t) - w(t-\Delta t)}\right]^2 + \left(\frac{3.8\,\nu}{u^2\Delta t}\right)^2 \left(\frac{w(t+\Delta t) + w(t-\Delta t) - 2\,w(t)}{w(t+\Delta t) - w(t-\Delta t)}\right)^2 \\ &\quad + \left(\frac{3.8\,\nu}{u^3}\right)^2 \left[\frac{u(t+\Delta t) - u(t-\Delta t)}{2\Delta t}\right]^2 + \frac{4u'^4 \int_o^\infty [f(r')/r']\,dr'}{\{[w(t+\Delta t) - w(t-\Delta t)]/2\Delta t\}^2} \end{aligned} \tag{38a}$$

where the assumed statistical independence of the three groups of terms requires that they contribute to $(\epsilon_{\partial/\partial x})^2$ as the sum of their squares. A review of the construction of $\epsilon_{\partial/\partial x}$ suggests that the several major approximations should lead to a conservative estimate for the uncertainty.

The full value of the uncertainty in $\epsilon_{\partial w/\partial x}$ can now be constructed. Specifically, the relationship for $\epsilon_{\partial/\partial x}$ from (38a) can be utilized in the expression for $\epsilon_{\partial w/\partial x}$ from (43). This lengthy expression will not be explicity written here.

An examination of equation (43) reveals that a portion of it may be calculated a priori; viz., $[\epsilon_u^2 + \epsilon_w^2]^{1/2}$. This quantity will be termed $\epsilon'_{\partial/\partial x}$; it is included in Figure 8 for reference purposes.

3.2.3.2. Uncertainty in $\partial u/\partial z$

The quantity $\partial u/\partial z$ will be constructed from two single wire probes which are parallel to the y axis, displaced a distance $2\Delta z$ apart, and located at a distance of Δy from the x-wire. The x-wire occupies the location of interest, viz., (x, y, z). The essential strategy of this measurement is to determine the desired quantity $\partial y/\partial z$ at x, y, z from the value

$$\frac{V(x, y+\Delta y, z+\Delta z) - V(x, y+\Delta y, z-\Delta z)}{2\Delta z} \cos \gamma(x, y, z) \qquad (51)$$

where the single wire is assumed to respond to the magnitude of the x-z plane velocity component. (Note: This assumption of the cosine relationship for the yaw (i.e., v) effects of the straight wires is justified on the basis that it is less restrictive than other assumptions which will necessarily be made.)

The measured quantity is an admixture of information from the y and the y + Δy planes; consequently, one element of the uncertainty is the magnitude of the ratio

$$\frac{V(x, y+\Delta y, z+\Delta z) - V(x, y+\Delta y, z-\Delta z)}{V(x, y, z+\Delta z) - V(x, y, z-\Delta z)} \qquad (52)$$

If the central difference value were an accurate method of constructing the derivative and if there were no uncertainty in assessing or utilizing cos γ, then

$$\frac{\partial u}{\partial z} = \frac{\partial u}{\partial z}\Big]_T [1 + \epsilon_{\Delta y} + \dots] \qquad (53)$$

would relax to

$$\frac{\partial u}{\partial z} = \frac{\partial u}{\partial z}\Big]_T [1 + \epsilon_{\Delta y}] \tag{53a}$$

Note that the numerator of (52) is the measured value whereas the denominator is equivalent to the true value for the stated conditions. Hence, the quantity $(1 + \epsilon_{\Delta y})$ is equal to the ratio given in (52). A rather simple procedure exists for the evaluation of this ratio; a four wire array with single wires parallel to the y axis will be made and the r.m.s. value of the ratio will be used to compute $\epsilon_{\Delta y}$. Namely,

$$\epsilon_{\Delta y} = \left\{ \frac{1}{T_o} \int_o^T \left[\frac{V(x, y+\Delta y, z+\Delta z) - V(x, y+\Delta y, z-\Delta z)}{V(x, y, z+\Delta z) - V(x, y, z-\Delta z)} \right]^2 dt \right\} - 1 \tag{54}$$

The motivation for using $\gamma(x, y, z)$ versus $\gamma(x, y, z+\Delta z)$ and $\gamma(x, y, z-\Delta z)$ is simply that the first value is available during the measurement of ω_y. An expression for the uncertainty associated with this aspect of the measurement can be developed as follows. Since $u = V \cos \gamma$

$$\frac{\partial u}{\partial z}\Big]_{x, y, z} = \frac{\partial}{\partial z} [V \cos \gamma]_{x,y,z}$$

$$= \cos \gamma \frac{\partial V}{\partial z}\Big]_{x, y, z} + V \frac{\partial \cos \gamma}{\partial z}\Big]_{x, y, z}$$

$$\cong \cos \gamma \frac{\partial V}{\partial z}\Big]_{x, y+\Delta y, z} [1 + \epsilon_{\Delta y}] + V \frac{\partial \cos \gamma}{\partial z}\Big]_{x, y, z} \tag{55}$$

where, the first term on the r.h.s. contains the measured quantity and the formulation

$$\frac{\partial u}{\partial z}\Big]_{\text{measured}} = \frac{\partial u}{\partial z}\Big]_T [+ \epsilon_{\Delta \cos} + \ldots] \tag{53b}$$

and a manipulation of (55)* allows the following definition of $\epsilon_{\Delta \cos}$

*Note that $\partial u/\partial z)_T$ is the $\partial u/\partial z$ on the lefthand side of (55).

$$\cos\gamma)_{x,y,z}\ \frac{\partial V}{\partial z})_{x,y+\Delta y,z} = \frac{\partial u}{\partial z}]_{x,y,z}\left[1 - \frac{V\frac{\partial \cos\gamma}{\partial z})_{x,y,z}}{\frac{\partial u}{\partial z})_{x,y,z}}\right]\left[\frac{1}{1+\epsilon_{\Delta y}}\right]$$

or

$$\epsilon_{\cos} \cong \frac{V\ \partial \cos\gamma/\partial z)_{x,y,z}}{\partial u/\partial z)_{x,y,z}} \tag{56}$$

An estimate of $\epsilon_{\cos}$ can be extracted from the data base used to evaluate the convective acceleration terms of the Taylor hypothesis. Namely, from two x-wire probes measuring u, w at (x, y-Δy, z-Δz) and (x, y+Δy, z+Δz) respectively, we can make the following approximations (recall that +Δ implies x, y+Δy, z+Δz and -Δ implies x, y-Δy, z-Δz):

$$\frac{u(+\Delta) - u(-\Delta)}{2\Delta z} = \left(\frac{\partial u}{\partial y} + \frac{\partial u}{\partial z}\right) \tag{57}$$

and

$$\frac{\cos\gamma(+\Delta) - \cos\gamma(-\Delta)}{2\Delta z} = \frac{\partial}{\partial y}\cos\gamma + \frac{\partial}{\partial z}\cos\gamma \tag{58}$$

By squaring and time averaging each side of (57) and (58), we obtain

$$<\left[\frac{u(+\Delta) - u(-\Delta)}{2\Delta z}\right]^2> = <\left[\left(\frac{\partial u}{\partial y}\right)^2 + 2\left(\frac{\partial u}{\partial y}\right)\left(\frac{\partial u}{\partial z}\right) + \left(\frac{\partial u}{\partial z}\right)^2\right]>$$

$$\cong \overline{2\left(\frac{\partial u}{\partial z}\right)^2} \tag{59}$$

and similarly

$$<\left[\frac{V(+\Delta) + V(-\Delta)}{2}\right]^2\left[\frac{\cos\gamma(+\Delta) - \cos\gamma(-\Delta)}{2\Delta z}\right]^2> \cong \overline{2\,V^2\frac{\partial \cos\gamma}{\partial z}} \tag{60}$$

where the rather major assumptions of local isotropy allows the approximations

$$\overline{\left(\frac{\partial u}{\partial y}\right)^2} = \overline{\left(\frac{\partial u}{\partial z}\right)^2} \quad \text{and} \quad \overline{\left(\frac{\partial u}{\partial y}\right)\left(\frac{\partial u}{\partial z}\right)} = 0 \tag{61}$$

and similarly for the (V cos γ) product. Note that $\langle[\ ]\rangle$ is used interchangeably with $\overline{[\ ]}$ for the time average of [ ]. Consequently, the output of the two x-wire arrays can be used to evaluate ϵ_{cos}. Specifically,

$$\epsilon_{cos} \simeq \left\{ \frac{1}{T} \int_o^T \left[\frac{V(+\Delta) + V(-\Delta)}{2} \quad \frac{\cos\gamma(+\Delta) - \cos\gamma(-\Delta)}{u(+\Delta) - u(-\Delta)} \right]^2 dt \right\}^{1/2} \tag{62}$$

It is somewhat discouraging to note that $[\cos\gamma(+\Delta) - \cos\gamma(-\Delta)]$ will have to be quite small in order to overcome the large multiplicative factor in the balance of ϵ_{cos}.

The cosine term itself also introduces some uncertainty; viz.,

$$\cos\gamma = \cos(\gamma_T + \delta\gamma)$$

and

$$\begin{aligned} \cos\gamma &= \cos\gamma_T \cos\delta\gamma - \sin\gamma_T \sin\delta\gamma \\ &\cong \cos\gamma_T - \delta\gamma \sin\gamma_T \\ &= \cos\gamma_T [1 - \delta\gamma \tan\gamma_T] \end{aligned}$$

or

$$\epsilon_{\cos\gamma} = \delta\gamma \tan\gamma \tag{63}$$

and $\epsilon_{\cos\gamma}$ can be calculated using the previously identified uncertainty parameters: $\Delta\gamma$, $\Delta V/V$ and v/V.

The separate measurements and/or calculations of the quantities $\epsilon_{\Delta y}$, ϵ_{cos}, $\epsilon_{\cos\gamma}$ require that they be combined as if they were statistically independent. Hence

$$\frac{\partial u}{\partial z}) = \cos\gamma) \frac{\partial V}{\partial z})_{x,\, y+\Delta y,\, z} = \frac{\partial u}{\partial z})_T [1 + \epsilon_{cos} + \epsilon_{\cos\gamma}][\frac{1}{1 + \epsilon_{\Delta y}}]$$

$$= \frac{\partial u}{\partial z}]_T [1 + \epsilon_{\partial u/\partial z}]$$

which serves to define the quantity $\epsilon_{\partial u/\partial z}$.

3.2.3.3. Statement of Uncertainty for ω_y

The separate evaluations of $\epsilon_{\partial u/\partial z}$ and $\epsilon_{\partial w/\partial y}$ can be collected to define ϵ_{ω_y}. Specifically,

$$\omega_y = \frac{\partial u}{\partial z} - \frac{\partial w}{\partial x}$$

$$= \frac{\partial u}{\partial z})_T + \delta\left(\frac{\partial u}{\partial z}\right) - \frac{\partial w}{\partial x})_T - \delta\left(\frac{\partial w}{\partial x}\right)$$

$$= \left\{ \frac{\partial u}{\partial z})_T - \frac{\partial w}{\partial x})_T \right\} \left\{ 1 + \frac{\delta\left(\frac{\partial u}{\partial z}\right)}{\frac{\partial u}{\partial z})_T - \frac{\partial w}{\partial x})_T} - \frac{\delta\left(\frac{\partial w}{\partial x}\right)}{\frac{\partial u}{\partial z})_T - \left(\frac{\partial w}{\partial x}\right)_T} \right\}$$

$$= \omega_y)_T \left\{ 1 + \frac{\frac{\partial u}{\partial z})_T \epsilon \frac{\partial u}{\partial z}}{\omega_y)_T} - \frac{\frac{\partial w}{\partial x})_T \epsilon \frac{\partial w}{\partial x}}{\omega_y)_T} \right\}$$

$$= \omega_y)_T \left\{ 1 + \epsilon_{\omega_y} \right\} \qquad (65)$$

It will be consistent with the approximate nature of the ϵ quantities to construct ϵ_{ω_y} using the (constant) values of $\epsilon_{\partial u/\partial z}$ and $\epsilon_{\partial w/\partial x}$ evaluated from the above described experimental data and calculations and multiply these by the measured $\partial u/\partial z$ and $\partial w/\partial x$ values.

REFERENCES

Brown, G. L. and Roshko, A., "On density effects and large structure in turbulent mixing layers," Jour. Fluid Mech., vol. 64, pp. 775-816 [1974].

Brunn, H. H., "Interpretation of a hot-wire signal using a universal calibration law," Jour. of Physics E., Scientific Instruments, vol. 4, pp. 225-231 [1971].

Champagne, F. H., Sleicher, C. A. and Whermann, O. H., "Turbulence measurements with inclined hot-wire, part 1," Jour. Fluid Mech., vol. 28, pp. 153-175 [1967].

Collis, D. C., and Williams, M. J., "Two-dimensional convection from heated wires at low Reynolds numbers," J. Fluid Mech., vol. 6, pp. 357-384 [1959].

Corrsin, S., and Kistler, A. L., "Free stream boundaries of turbulent flows," NACA Rept. 1244 [1955].

Foss, J. F., "Vorticity and acoustics measurements in impinging jet flows, part I," Second Semi-Annual Report, NASA Langley Research Center, Grant No. NGR 23-004-091, June [1975].

Foss, J. F., and Kleis, S. J., "Mean flow characteristics for the olbique impingement of an axisymmetric jet," AIAA Journal Synoptic [1976], accepted for publication.

Friehe, C. A., and Schwarz, W. H., "Deviations from the cosine law for yawed cylindrical hot-wire sensors," Jour. Applied Mech., Trans. ASME, vol. 35, pp. 655-662 [1968].

Fujita, H., and Kovasznay, L. S. G., "Measurement of Reynolds stress by a single rotated hot-wire anemometer," Rev. of Scientific Inst., vol. 39, No. 9, p. 1351 [1968].

Hardin, J. C., "Analysis of noise produced by an orderly structure of turbulent jets," NASA TN D-7242, April [1973].

Hinze, J. O., Turbulence, McGraw-Hill Book Co., [1959].

Kistler, A. L., "The vorticity meter," M.S. Thesis, The Johns Hopkins University [1952].

Lighthill, M. J., "Introduction: Real and Ideal Fluids," Laminar Boundary Layers, ed. L. Rosenhead, Oxford Univ. Press [1963].

Moore, D. W., and Saffman, P.B., "The density of organized vortices in a turbulent mixing layer," J. Fluid Mech., vol. 69, pp. 465-473 [1975].

Potter, M. C., and Foss, J. F., Fluid Mechanics, Ronald Press [1975].

Strohl, A., and Comte-Bellot, G., "Aerodynamic effects due to configuration of x-wire anemometers," Jour. Applied Mech., pp. 661-666 [1973].

Tennekes, H., and Lumley, J. L., A First Course in Turbulence, MIT Press, Cambridge, Mass. [1972].

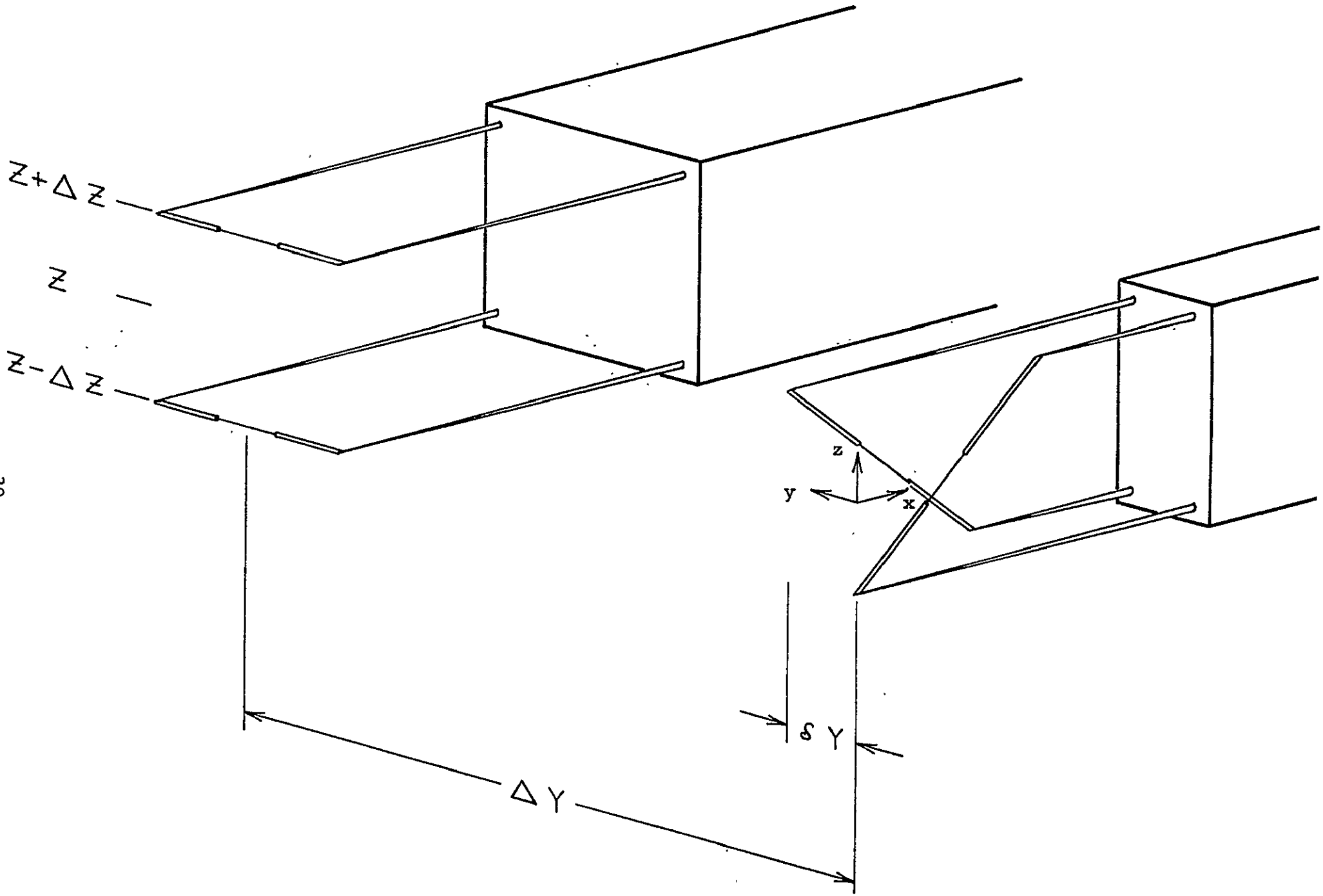

Figure 1. Definition sketch for the probe response analysis of Section 1.
(Note: actual probe body will be streamlined)

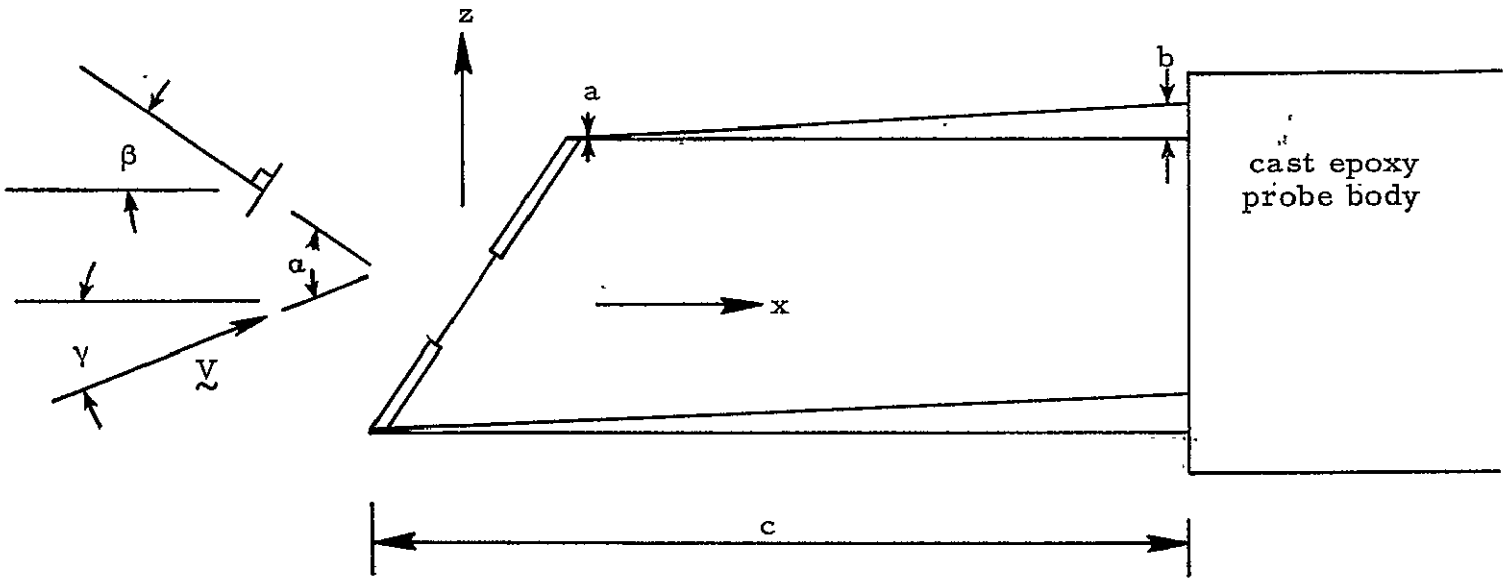

Notes: a = 0.2 mm α ≃ 45 degrees
b = 0.4 mm active portion of wire 5 μ dia., 1 mm length
c = 2.0 mm total length of wire ~ 3 mm

Probe design based upon recommendations of Strohl and Comte-Bellot [1973].

Figure 2. Probe characteristics and definition of angles.

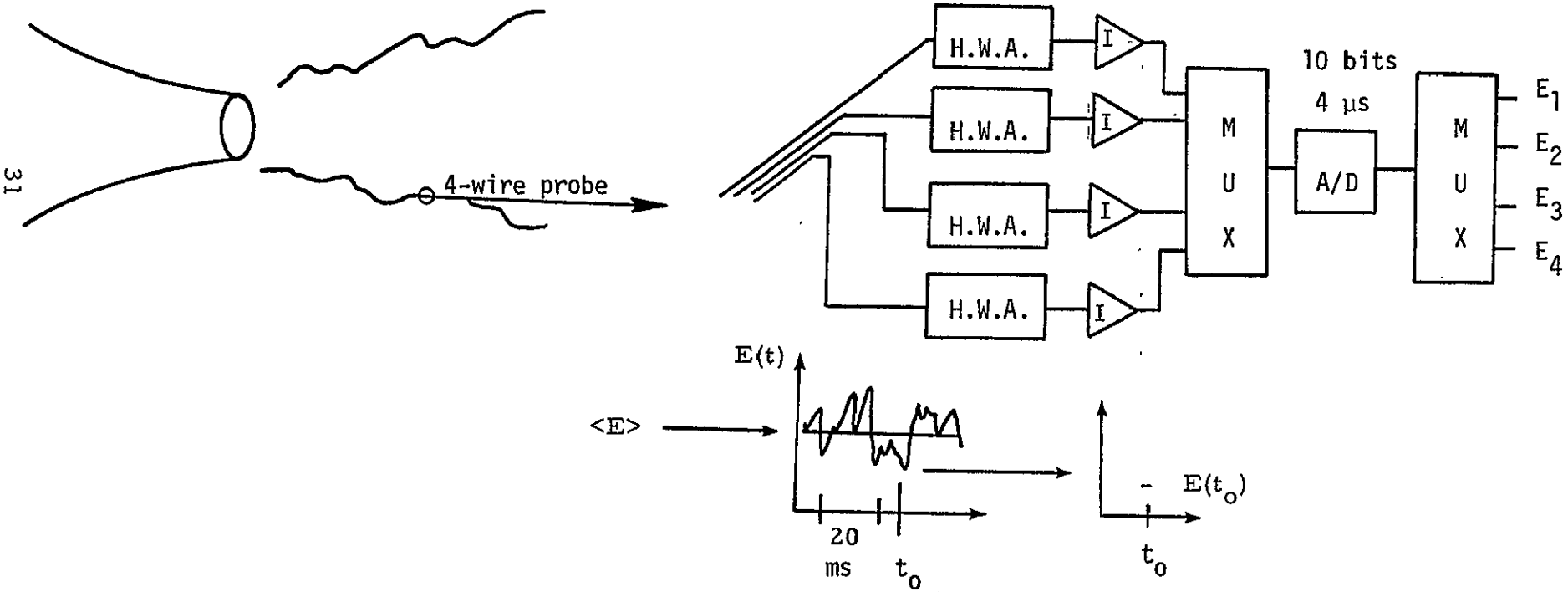

Note: Analog integrators: $\int_{t_o - \tau/2}^{t_o + \tau/2} E(t)\, dt$ where τ = 18.5, 23.1, 30.8, 46.2, 92.5 μsec. Equivalent frequencies, including capacitor discharge time, are 50, 40, 30, 20, 10 Khz.

Figure 3a. Analog processing of the hot-wire signals.

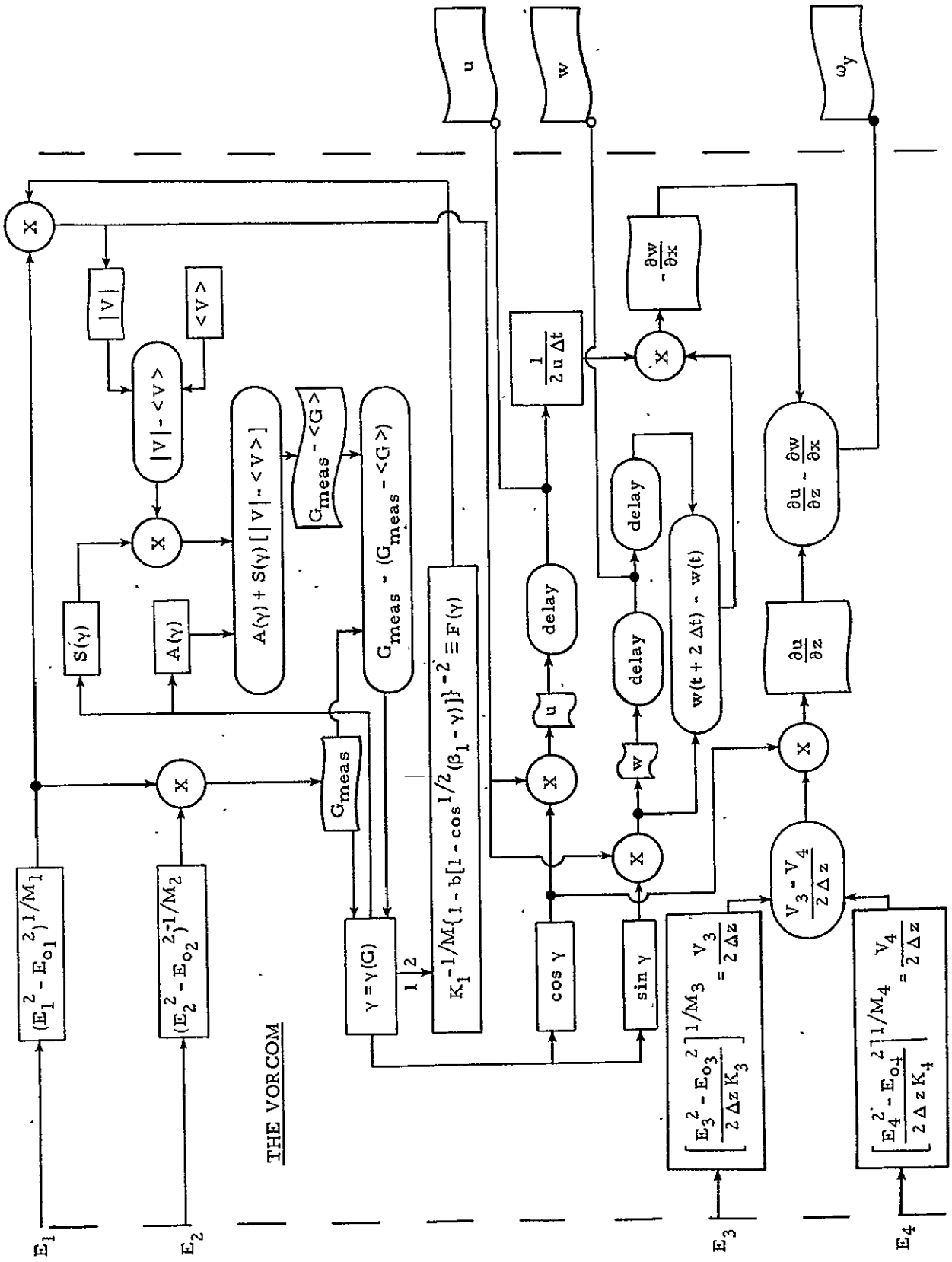

Figure 3b. The VORCOM.

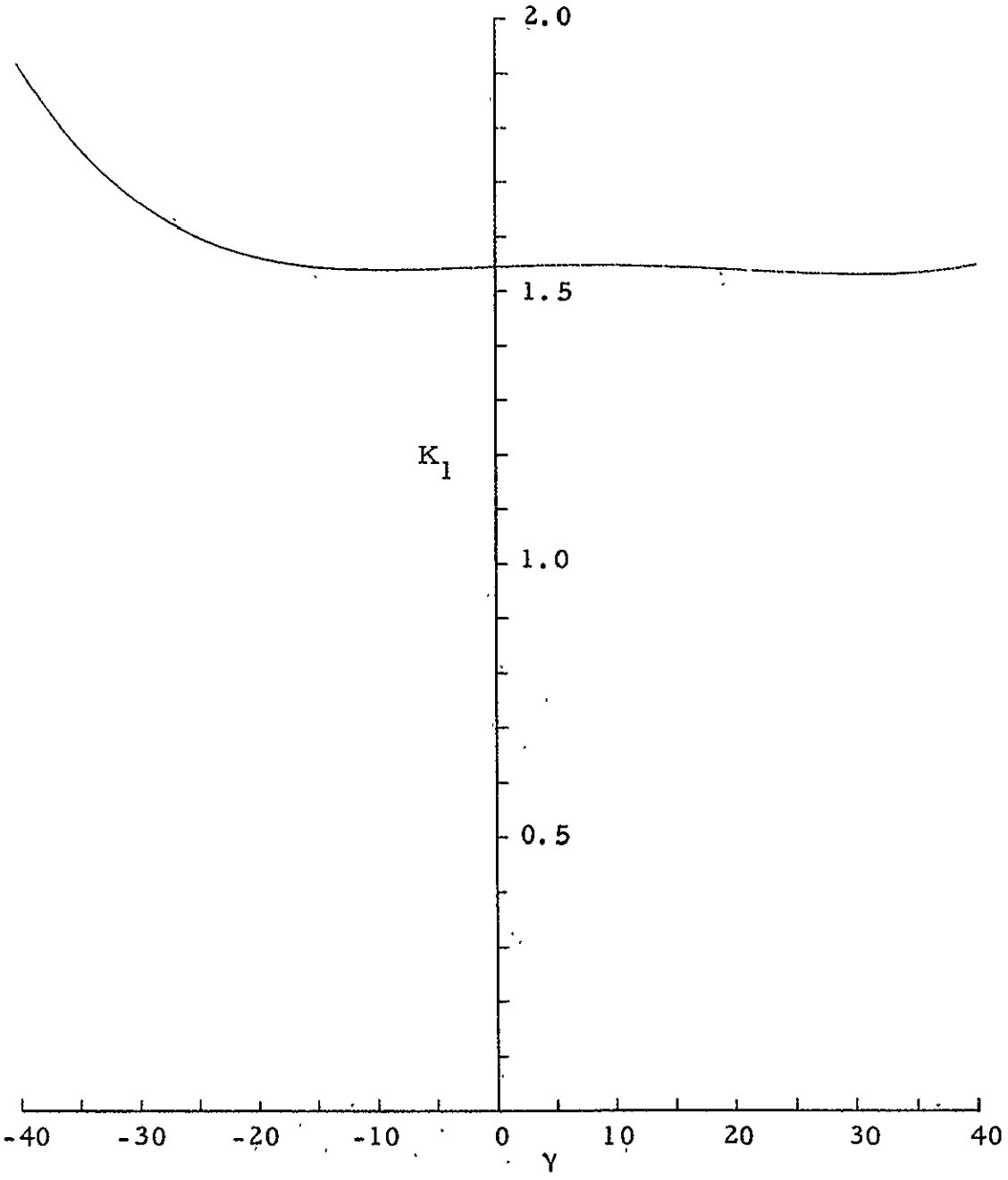

Figure 4. $K_1(\gamma)$ (see equation 13).

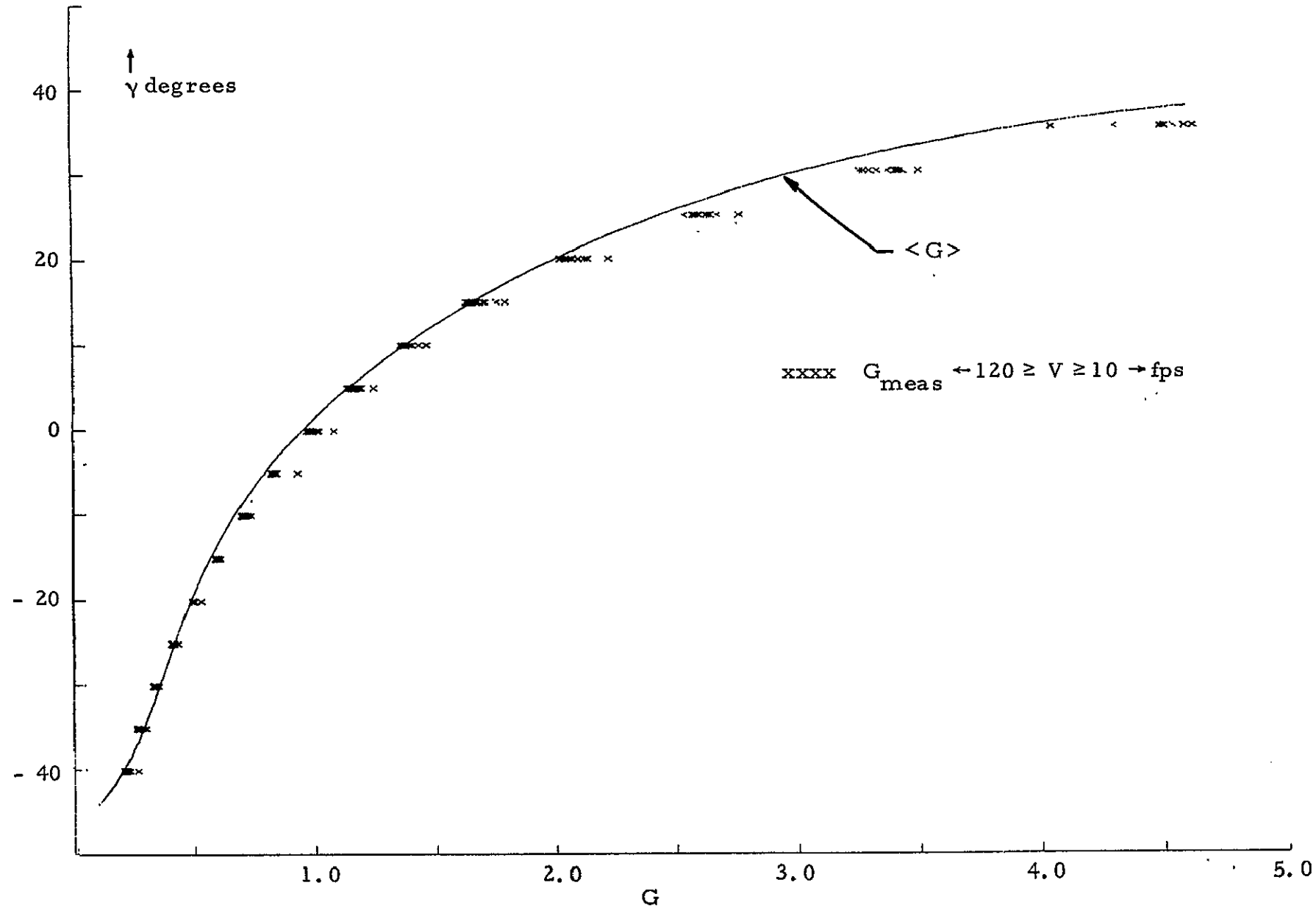

Figure 5. G(γ) (see equation 14).

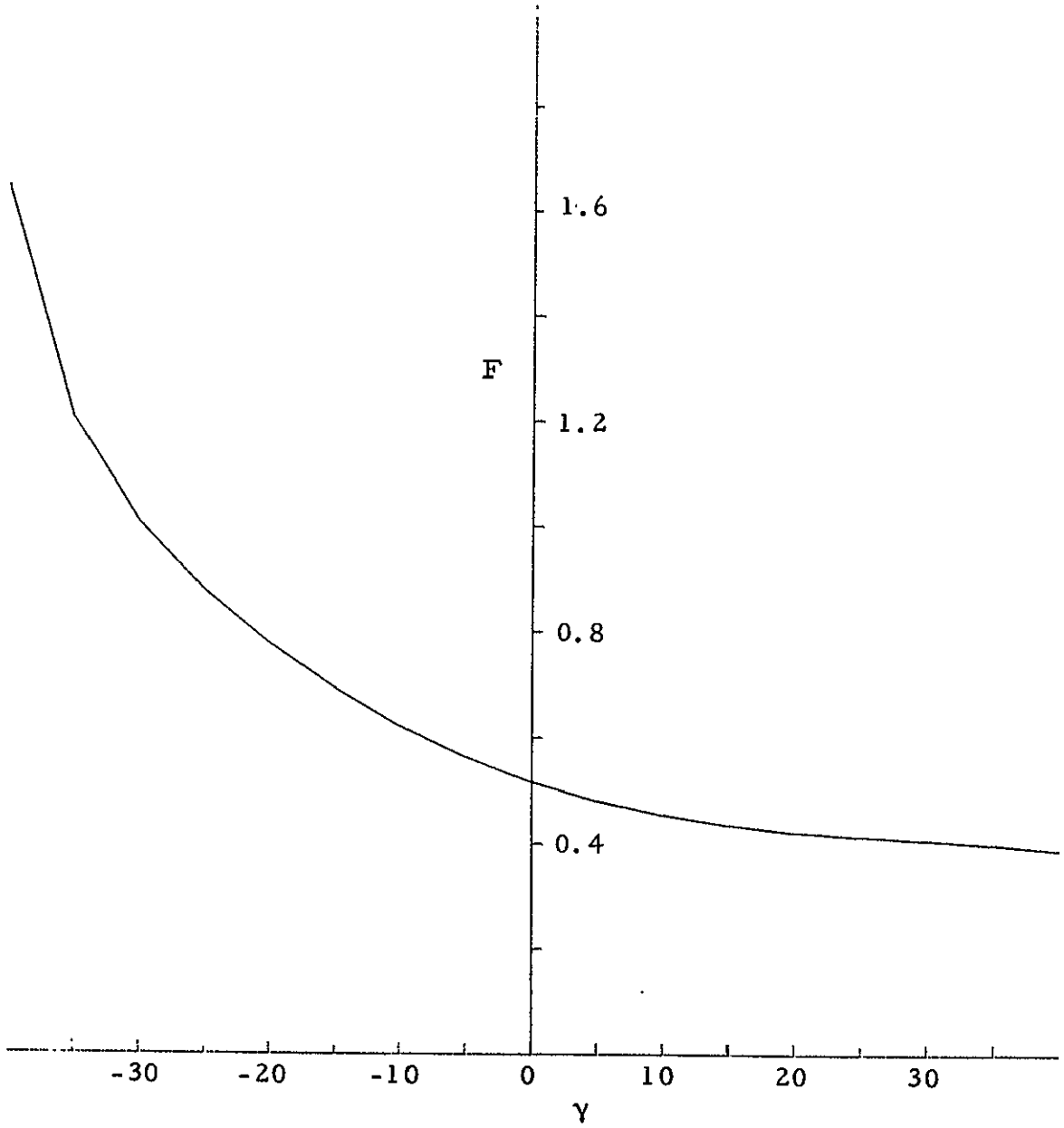

Figure 6. F(γ) (see equation 15 and 16).

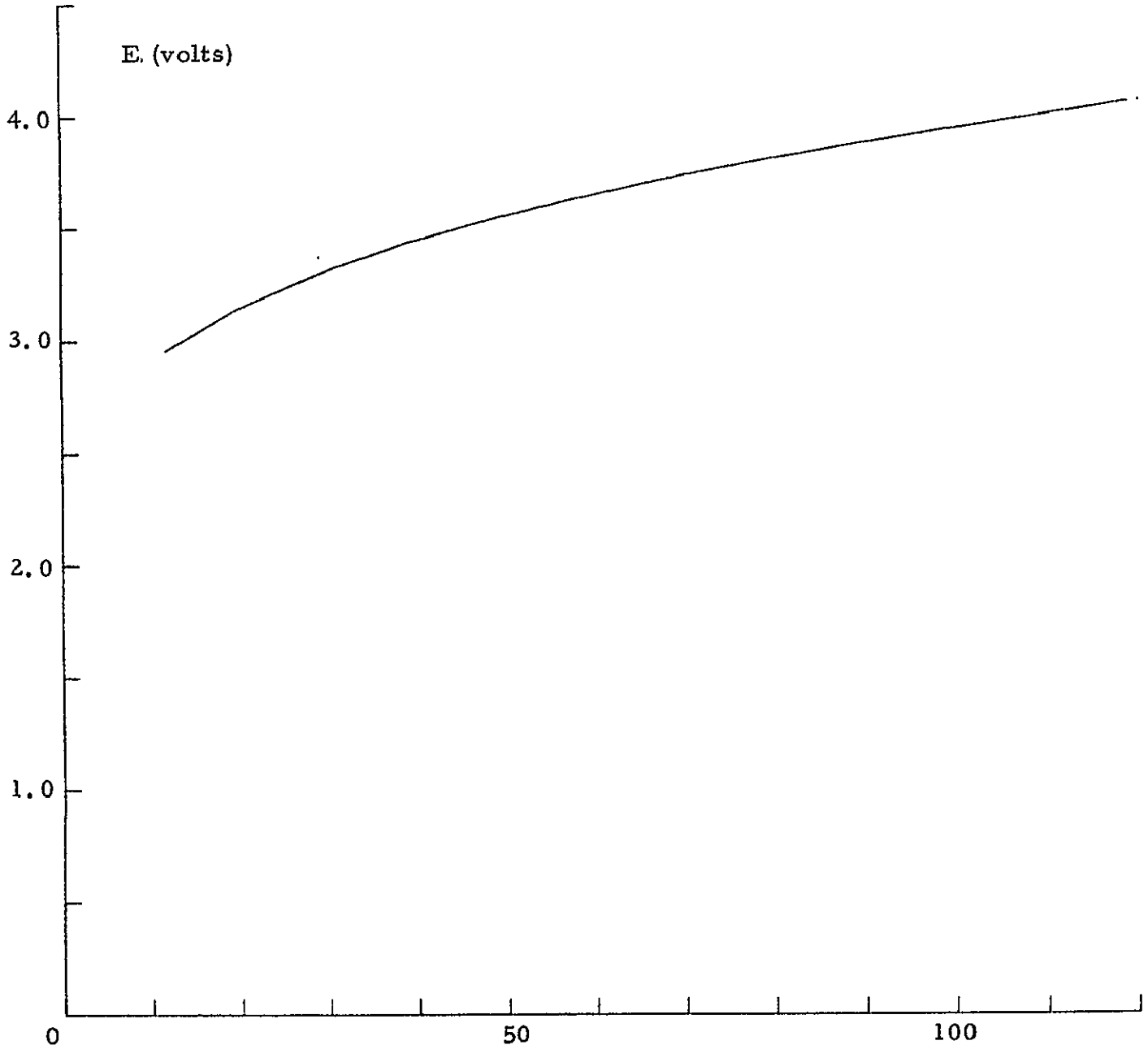

Figure 7a. E versus V, hot-wire calibration.
Note: Straight lines drawn through the discrete data points of Table 2 constitute the "curve" which is shown.

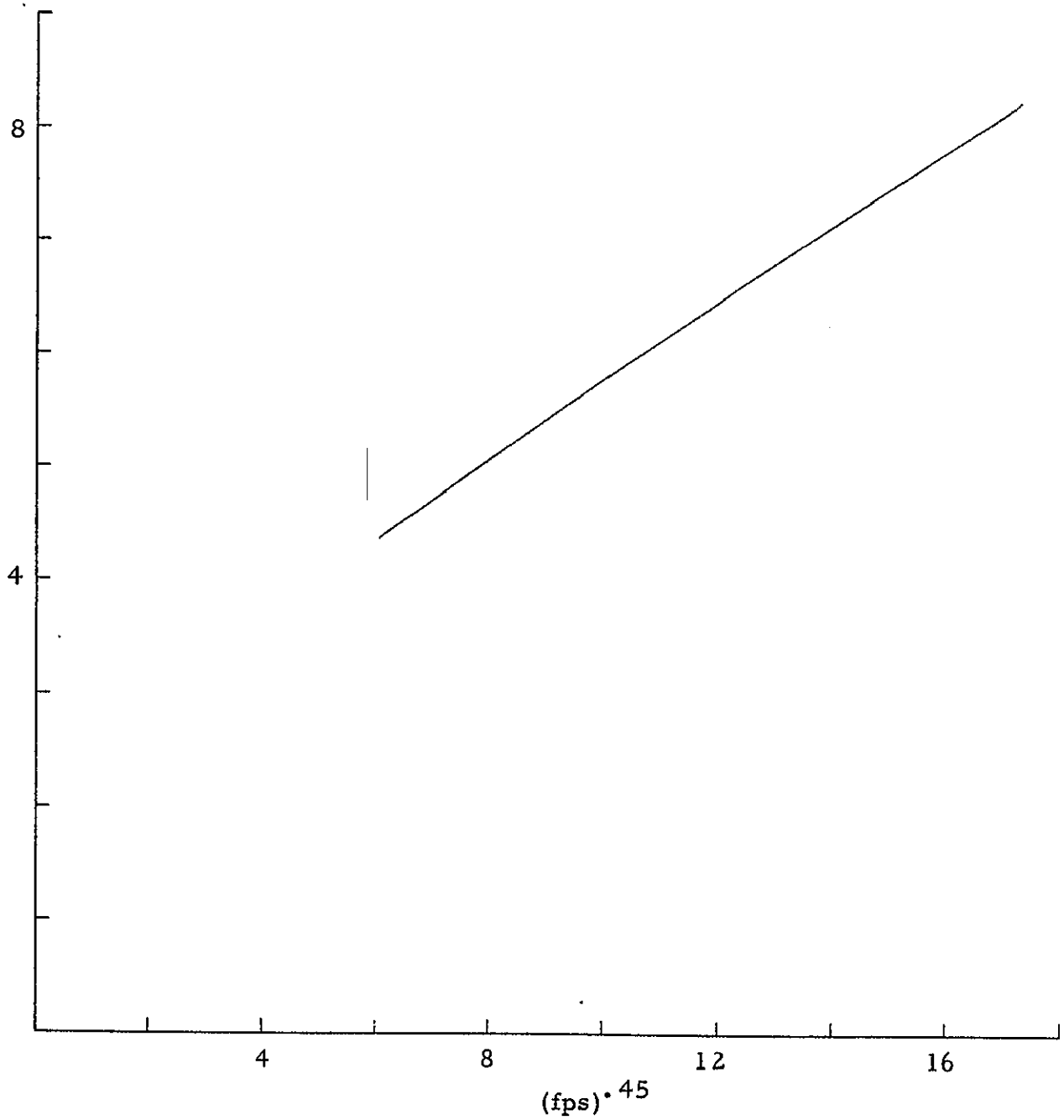

Figure 7b. E^2 versus V^m, m = 0.45

Note: Straight line segments have been drawn through the processed discrete data points of Table 2.

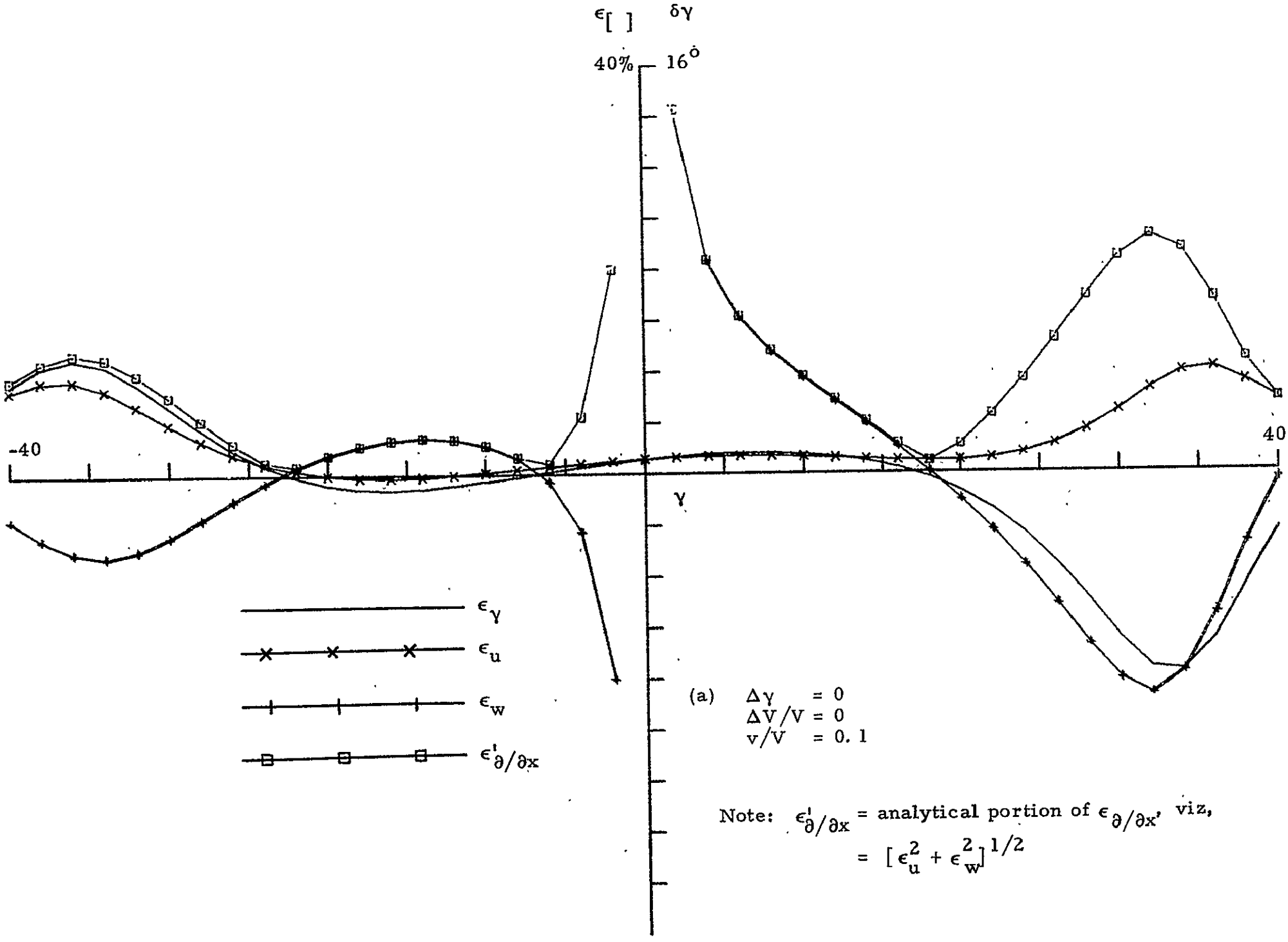

Figure 8. Representative results from the uncertainty analysis.

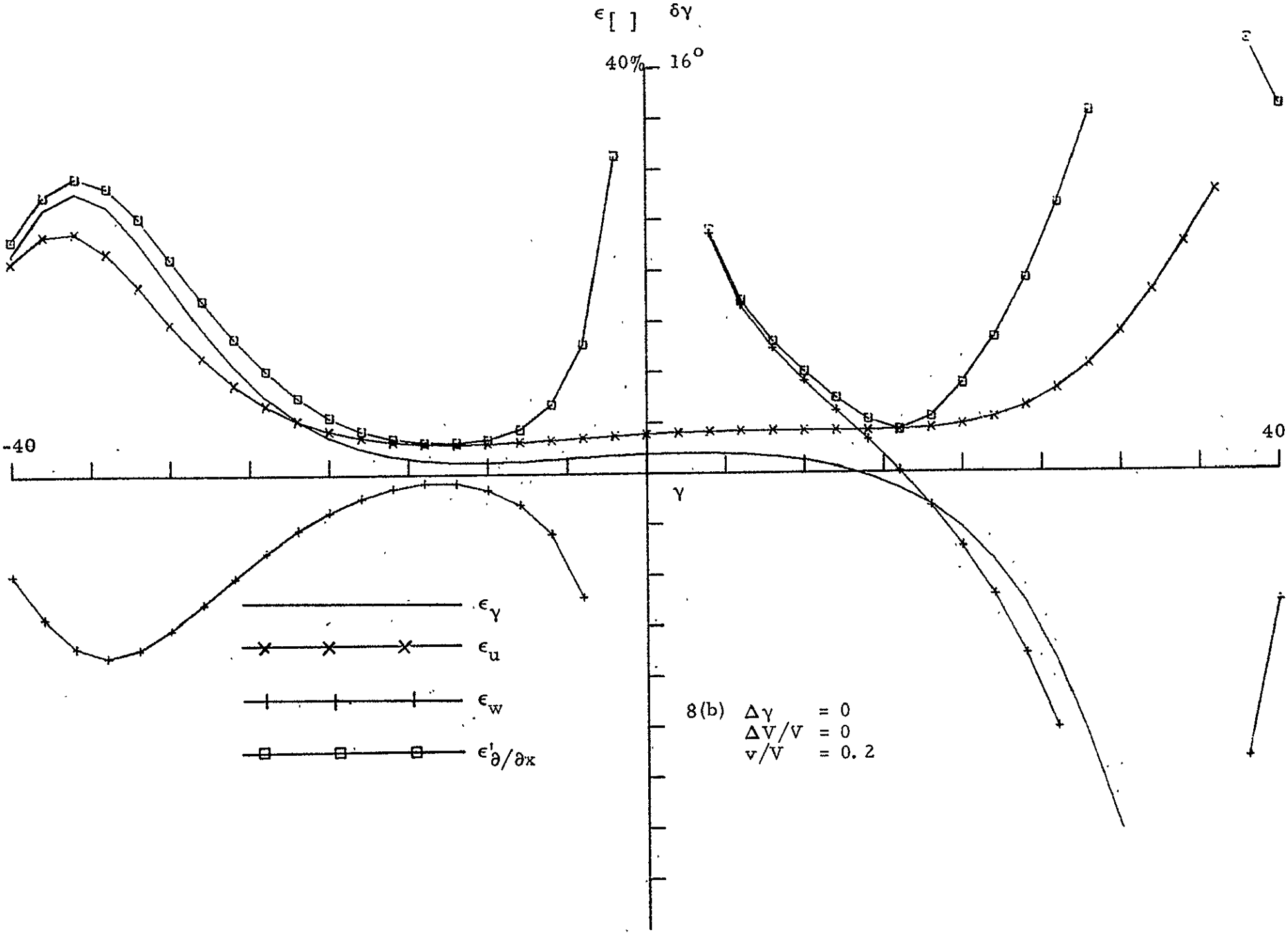
ϵ[ ]
$\delta\gamma$
40%
16°
-40
40
γ
ϵ_γ
ϵ_u
ϵ_w
$\epsilon'_{\partial/\partial x}$
8(b) $\Delta\gamma$ = 0
$\Delta V/V$ = 0
v/V = 0.2

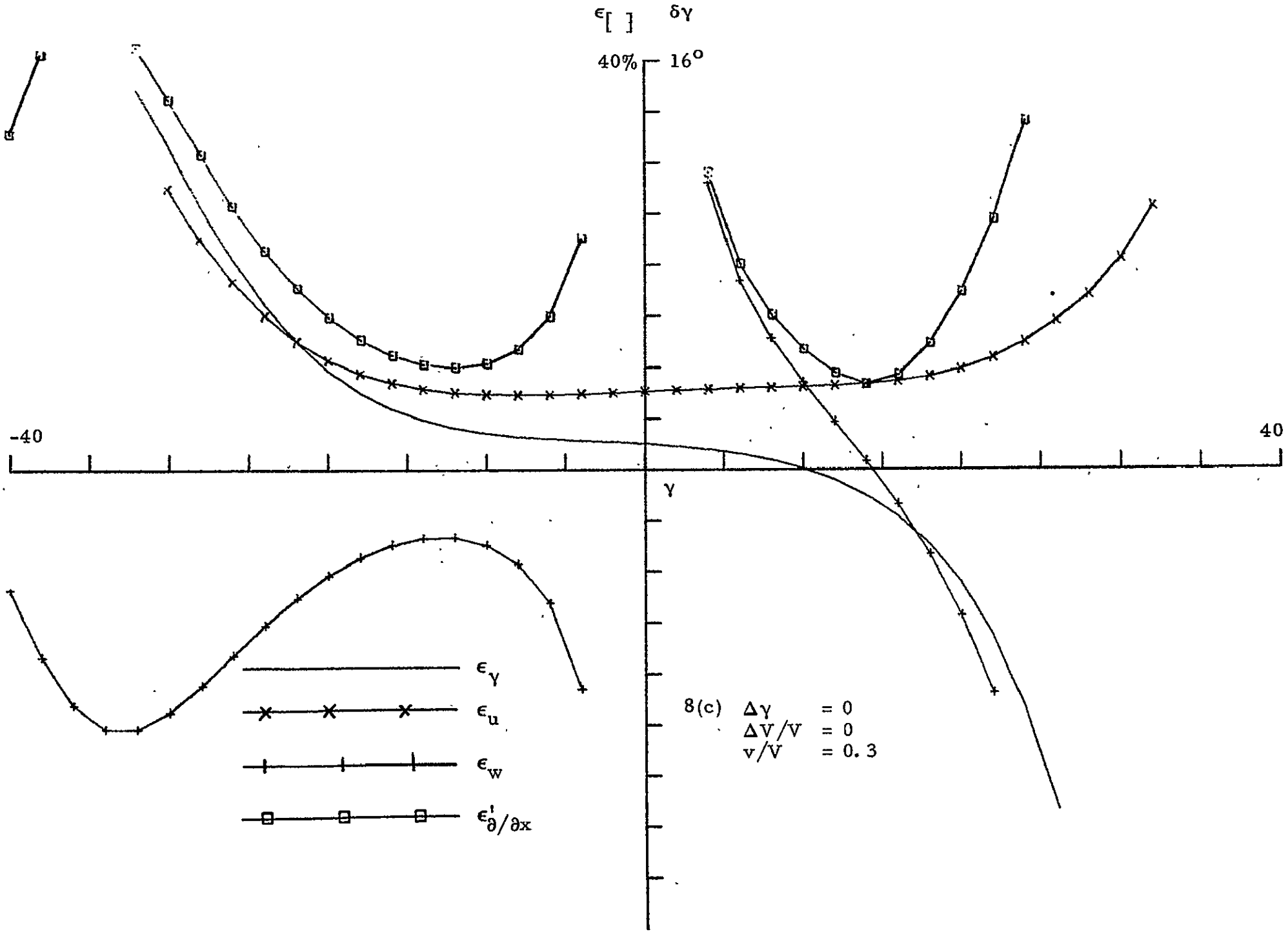
ϵ[ ]
$\delta\gamma$
40%
16°
-40
40
γ
40
ϵ_γ
ϵ_u
ϵ_w
$\epsilon'_{\partial/\partial x}$
8(c) $\Delta\gamma$ = 0
$\Delta V/V$ = 0
v/V = 0.3

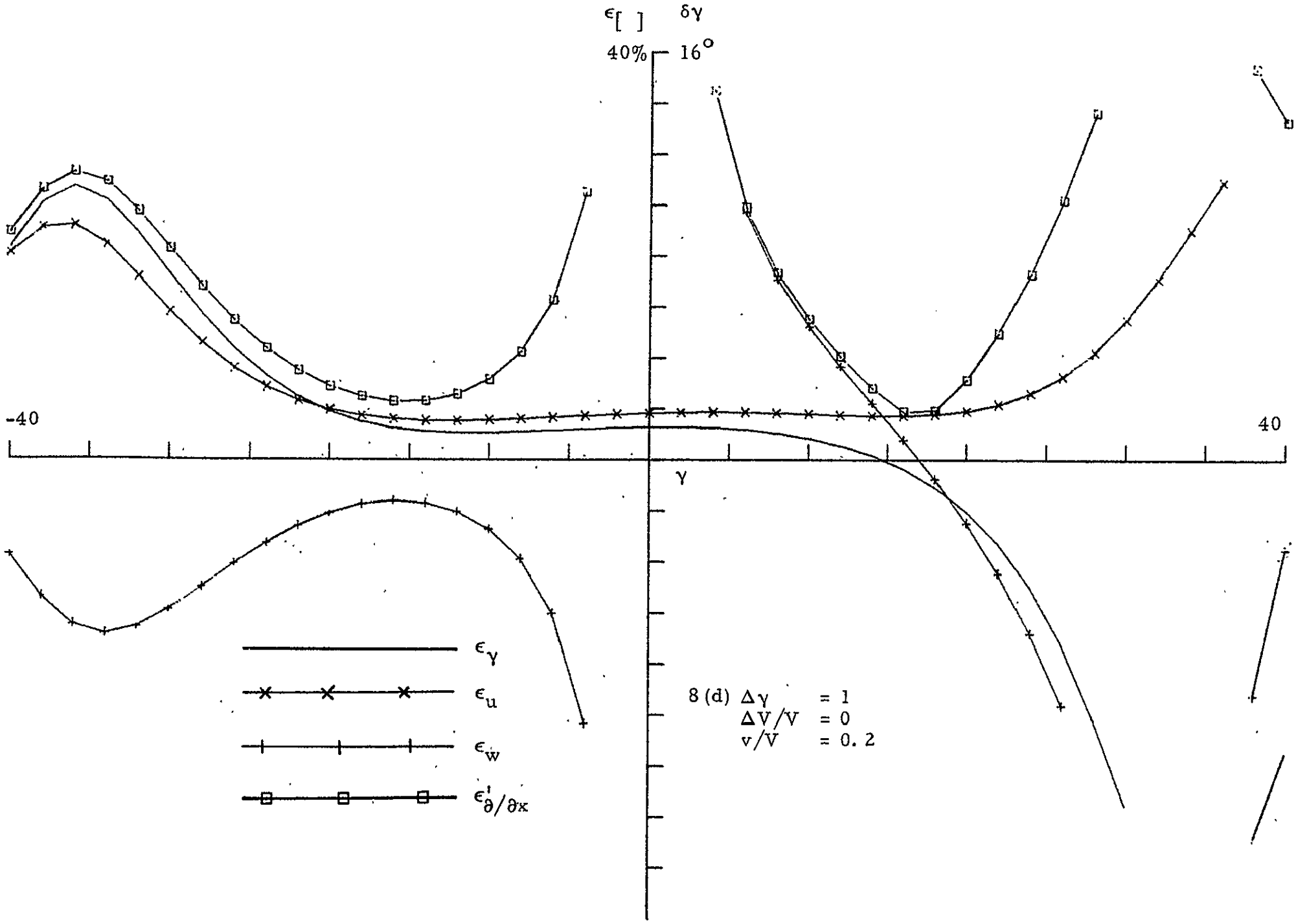
ϵ[ ]
40%
δγ
16°
-40
40
γ
ϵ_γ
ϵ_u
ϵ_w
$\epsilon'_{\partial/\partial x}$
8 (d) Δγ = 1
ΔV/V = 0
v/V = 0.2

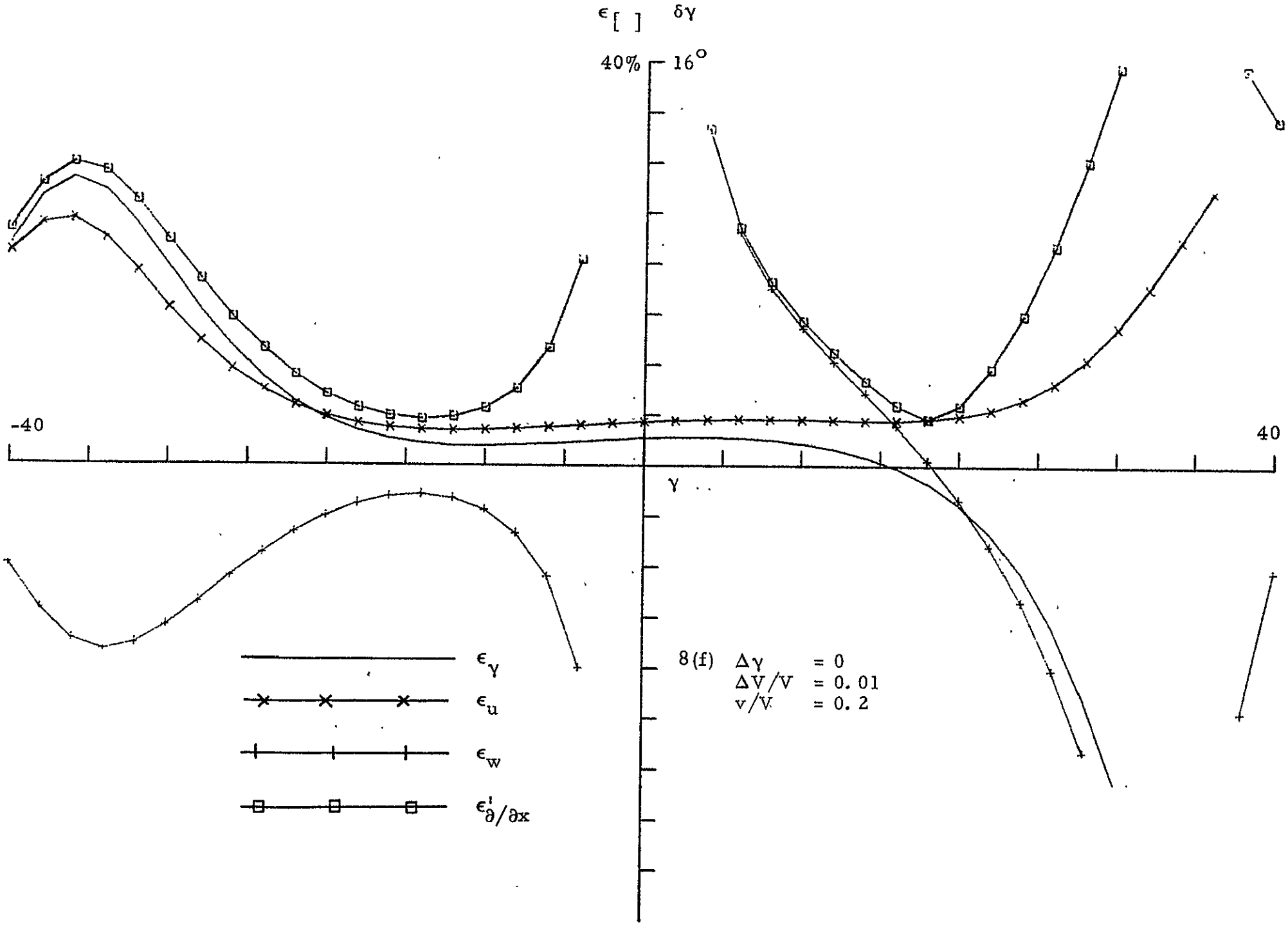
$\epsilon_{[\ ]}$ $\delta\gamma$
40%
16°
-40
40
γ
ϵ_γ
ϵ_u
ϵ_w
$\epsilon'_{\partial/\partial x}$
8(f) $\Delta\gamma$ = 0
$\Delta V/V$ = 0.01
v/V = 0.2

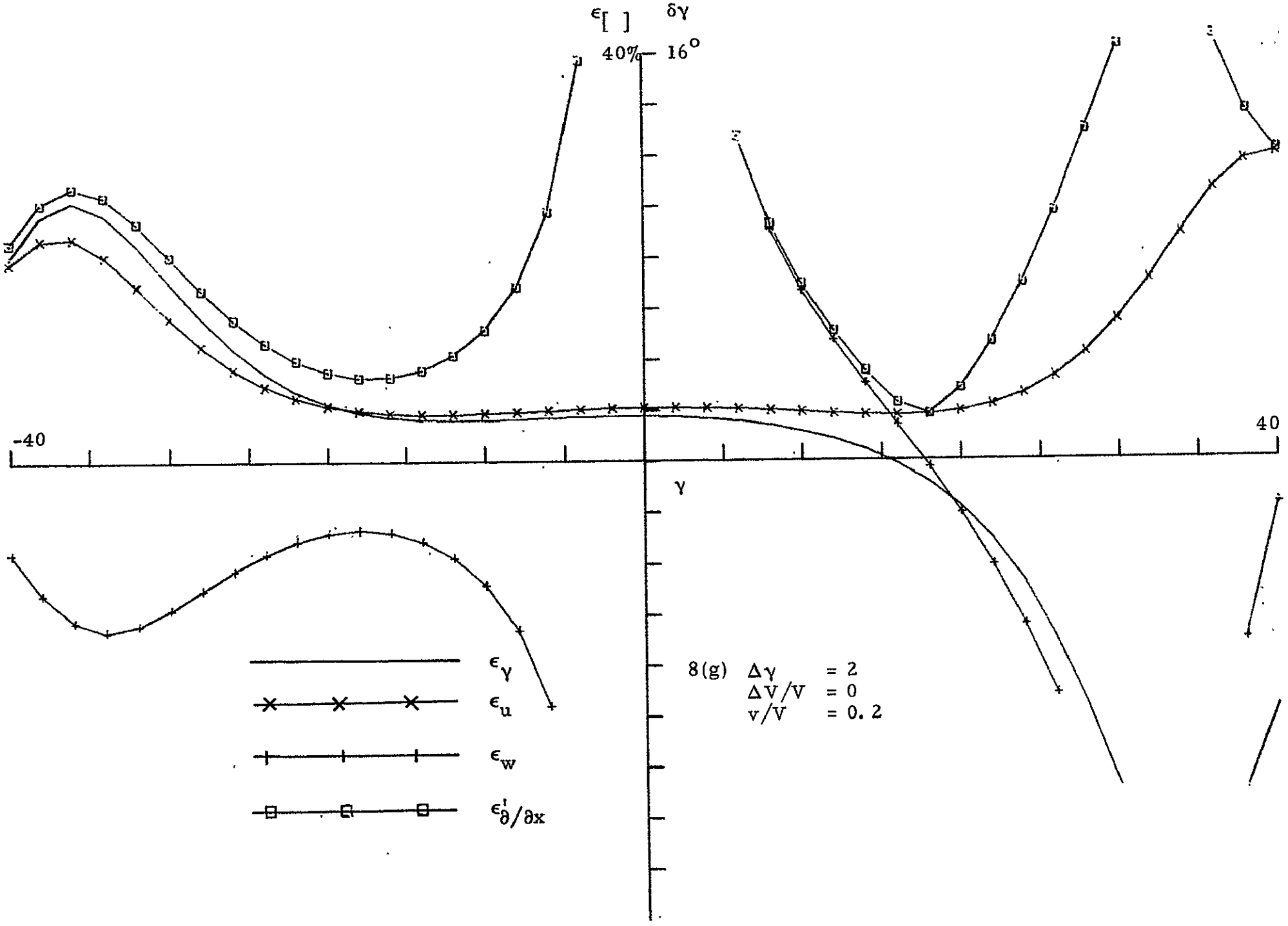
$\epsilon_{[\ ]}$
$\delta\gamma$
40%
16°
-40
40
γ
ϵ_γ
ϵ_u
ϵ_w
$\epsilon'_{\partial/\partial x}$
8(g) $\Delta\gamma$ = 2
$\Delta V/V$ = 0
v/V = 0.2

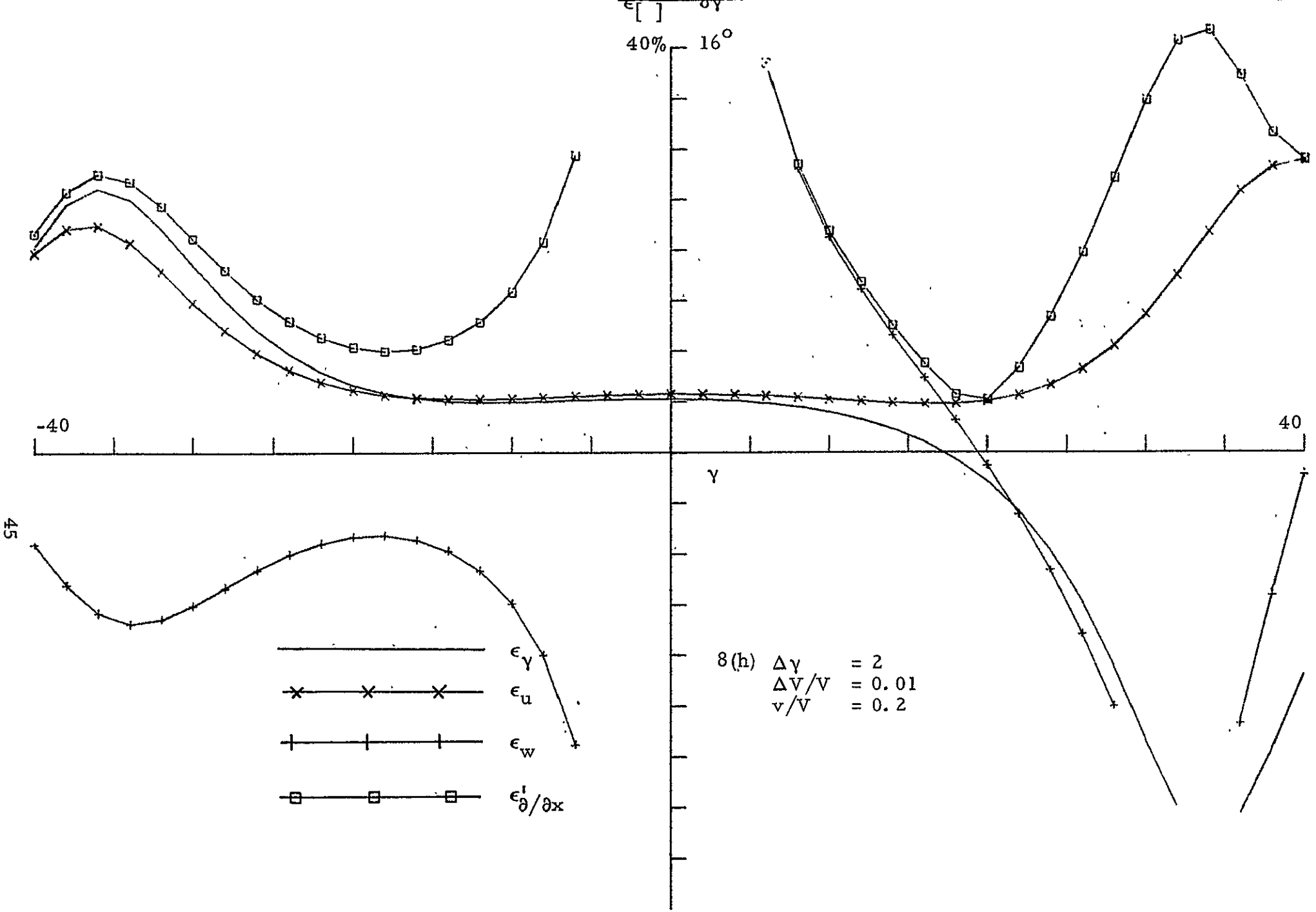
$\epsilon_{[\ ]}$ $\partial\gamma$
40%
16°
-40
40
γ
45
ϵ_γ
ϵ_u
ϵ_w
$\epsilon'_{\partial/\partial x}$
8(h) Δγ = 2
ΔV/V = 0.01
v/V = 0.2

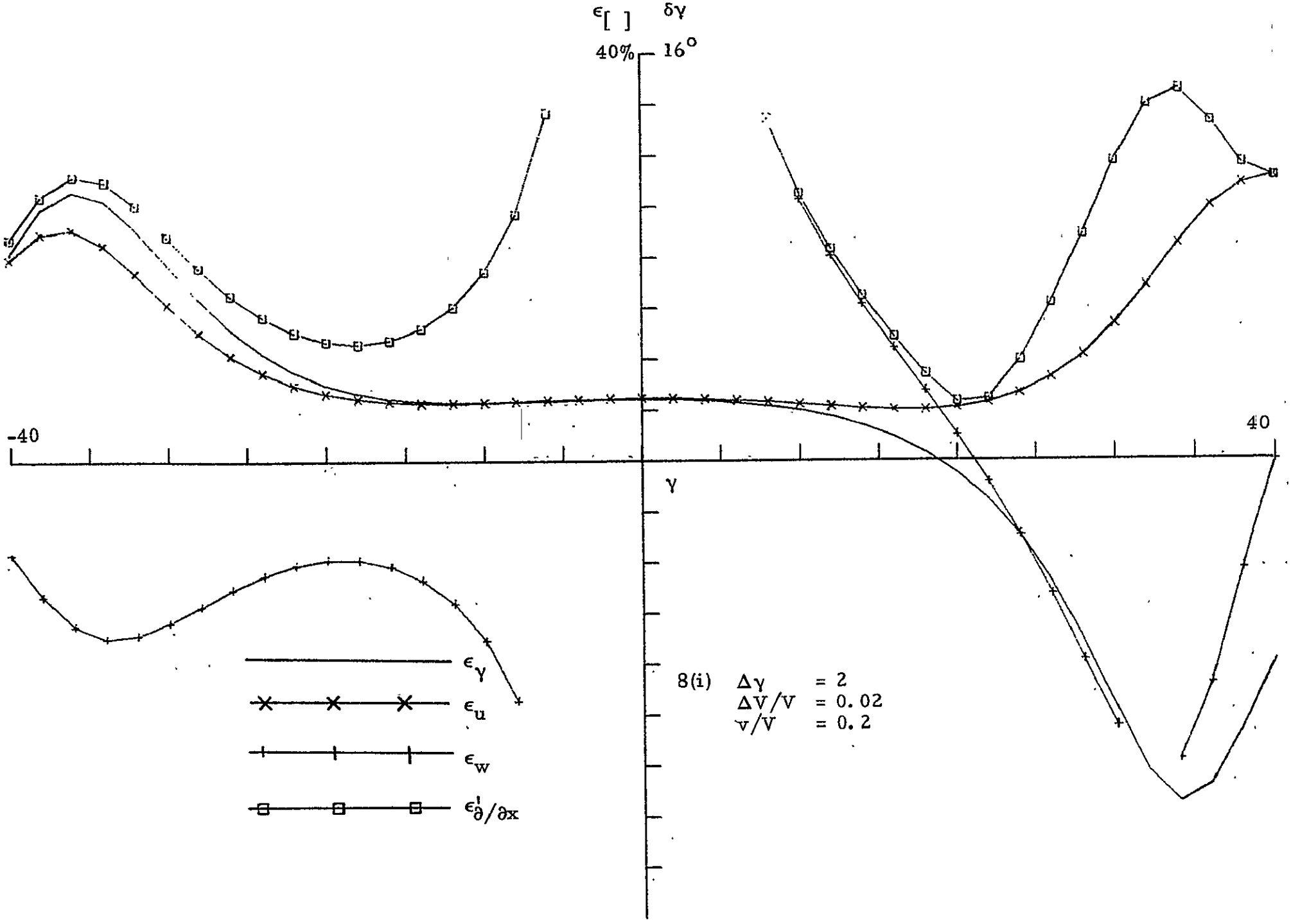
ϵ[ ]
40%
δγ
16°
-40
40
γ
ϵ_γ
ϵ_u
ϵ_w
$\epsilon_{\partial'/\partial x}$
8(i) Δγ = 2
ΔV/V = 0.02
v/V = 0.2

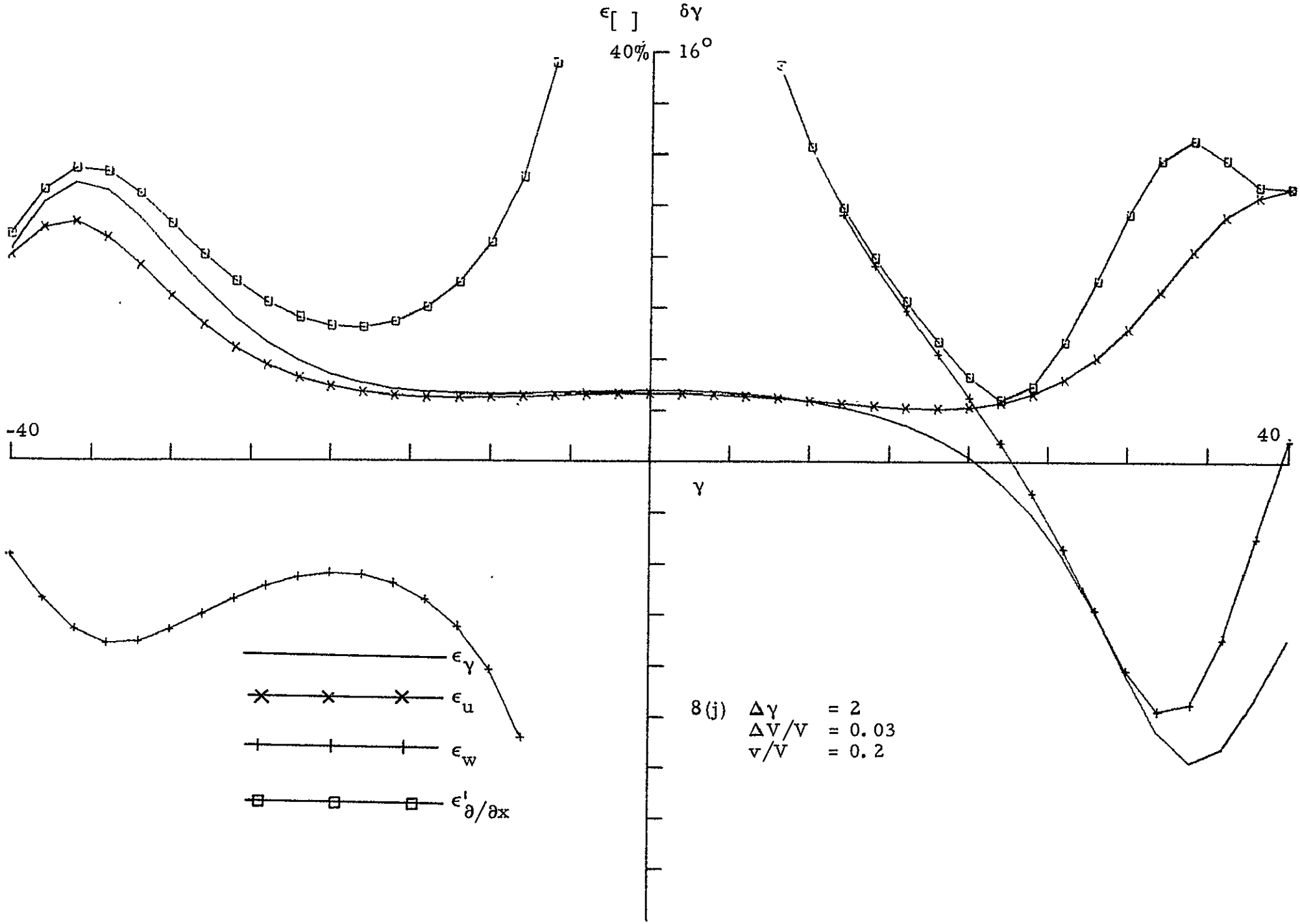
$\epsilon_{[\ ]}$
$\delta\gamma$
40%
16°
-40
40
γ
ϵ_γ
ϵ_u
ϵ_w
$\epsilon'_{\partial/\partial x}$
8(j) $\Delta\gamma$ = 2
$\Delta V/V$ = 0.03
v/V = 0.2

Table 1. "Constants" for the γ Computation Given E_1 and E_2 Values.

GAMMA	A	S	SD	(DGAM/DG)*SD
-40	1.26E-2	-8.47E-5	1.07E-2	5.18E-1
-35	-2.51E-2	-1.63E-5	6.81E-3	7.34E-1
-30	-2.98E-2	9.27E-5	2.52E-3	2.00E-1
-25	-1.84E-2	1.07E-4	2.80E-3	2.16E-1
-20	-4.53E-3	9.42E-5	9.32E-3	6.24E-1
-15	7.03E-3	1.11E-4	4.44E-3	2.44E-1
-10	1.48E-2	6.62E-5	2.70E-3	1.20E-1
- 5	1.57E-2	-1.16E-4	1.59E-2	5.68E-1
0	1.03E-2	-2.11E-4	8.49E-3	2.46E-1
5	-2.16E-2	-8.39E-5	1.02E-2	2.42E-1
10	-3.99E-2	-1.99E-4	1.12E-2	2.18E-1
15	-5.67E-2	-3.03E-4	8.07E-3	1.29E-1
20	-3.10E-2	-3.49E-4	9.69E-3	1.26E-1
25	2.26E-2	8.56E-5	2.27E-2	2.29E-1
30	1.23E-1	1.61E-3	7.09E-2	5.08E-1
35	1.48E-1	5.54E-3	1.95E-1	8.05E-1
40	-8.54E-1	1.55E-2	3.60E-1	-5.19E-1

Notes: (1) A and S are defined by the expression:

$$\langle G(\gamma) \rangle - G_{meas} = A(\gamma) + S(\gamma)[V - \langle V \rangle] ;$$

see equation (14) for the definition of G.

(2) SD = standard deviation between actual $\langle G \rangle - G_{meas}$ and values evaluated from the linear equation.

(3) Sensitivity of γ to errors of the linear equation is given by

$$\gamma_{error} = (DGAM/DG) * SD$$

Table 2. Calibration Data for x-wire Probe Array.

VEL	WIRE 1	WIRE 2
1.21030E 02	4.04599E 00	4.38013E 00
1.07906E 02	3.97028E 00	4.30451E 00
9.33095E 01	3.88373E 00	4.22596E 00
7.96535E 01	3.79260E 00	4.14354E 00
6.71927E 01	3.70110E 00	4.05441E 00
5.29811E 01	3.57423E 00	3.94312E 00
3.96047E 01	3.43806E 00	3.80764E 00
2.58724E 01	3.25336E 00	3.63442E 00
1.19316E 01	2.96599E 00	3.37164E 00
1.91827E 01	3.12629E 00	3.53613E 00
3.28003E 01	3.35071E 00	3.73504E 00
4.73371E 01	3.52301E 00	3.88813E 00
6.13657E 01	3.65531E 00	4.00981E 00
7.42294E 01	3.75814E 00	4.10600E 00
8.83925E 01	3.85291E 00	4.20058E 00
1.01225E 02	3.93376E 00	4.27257E 00
1.15125E 02	4.01068E 00	4.34596E 00
STAND DEV	4.37815E-01	5.50605E-01
EO**2	4.74595E 00	7.27388E 00
M	4.49572E-01	4.49399E-01

Note: Stand Dev (standard deviation) is based upon V_{calc} from $E^2 = E_o^2 + K V^m$ and V_{meas} from pressure transducer. m and E_o^2 from least squares routine.

PERCENT ERROR ON V_γ

VEL	-40.	-35.	-30.	-25.	-20.	-15.	-10.	-5.	0.	5.	10.	15.	20.	25.	30.	35.	40.
120.	0.3	-1.0	0.4	-0.4	1.2	1.1	1.0	0.6	0.4	0.4	0.1	0.1	0.0	-0.5	-0.8	0.0	1.4
110.	3.6	1.2	1.7	0.6	2.1	1.1	1.9	1.7	2.0	1.3	1.6	1.0	0.8	0.4	0.1	0.8	2.2
100.	-0.8	-0.4	1.5	0.2	0.5	2.0	2.0	1.2	1.4	0.8	0.9	1.0	0.2	-0.2	-0.6	0.1	1.5
90.	0.4	1.0	-0.7	0.8	1.3	1.6	1.6	1.5	1.4	0.2	0.2	0.6	-0.1	-0.8	-0.9	-0.6	1.2
80.	-0.3	0.9	-0.6	-0.4	0.9	1.4	1.3	1.0	0.0	0.7	0.4	0.0	-0.6	-0.9	-1.3	-0.7	0.7
70.	-0.4	-0.4	-0.2	0.1	-0.1	0.2	0.9	0.5	-0.2	0.4	0.1	-0.6	-0.6	-1.3	-1.6	-1.0	0.4
60.	-0.2	-1.3	-0.7	-1.2	0.0	0.6	0.1	0.2	0.5	0.0	-0.4	-0.2	-1.3	-1.6	-1.9	-1.3	0.0
50.	-1.9	-2.0	-0.1	0.2	0.0	0.1	0.0	0.1	0.6	-0.3	-0.3	-0.6	-1.1	-2.0	-2.1	-1.6	-0.8
40.	-1.2	-0.3	-0.9	0.5	0.1	0.7	0.6	0.5	0.2	0.0	0.0	-0.4	-0.8	-1.8	-2.7	-1.9	-1.2
30.	1.0	0.5	0.0	-0.2	-0.1	0.3	0.2	1.0	0.8	0.7	-0.2	0.1	-0.9	-1.6	-2.3	-1.8	-1.3
20.	1.5	1.8	2.1	1.1	2.2	3.1	2.5	2.2	2.9	1.7	2.0	0.8	0.1	-0.9	-1.1	-1.5	-1.0
10.	4.2	4.9	3.9	7.0	6.4	6.4	6.1	7.7	7.0	9.6	7.6	7.6	4.3	3.1	2.9	4.4	5.2

DIFFERENCE ON V (FPS)

VEL	-40.	-35.	-30.	-25.	-20.	-15.	-10.	-5.	0.	5.	10.	15.	20.	25.	30.	35.	40.
120.	-0.4	1.3	-0.5	0.5	-1.4	-1.3	-1.3	-0.7	-0.5	-0.5	-0.2	-0.2	0.0	0.6	1.0	0.0	-1.7
110.	-4.1	-1.4	-1.9	-0.7	-2.4	-1.2	-2.2	-1.9	-2.2	-1.5	-1.8	-1.2	-0.9	-0.4	-0.1	-0.9	-2.5
100.	0.8	0.4	-1.5	-0.2	-0.5	-2.0	-2.0	-1.2	-1.4	-0.8	-0.9	-1.0	-0.2	0.2	0.6	-0.1	-1.5
90.	-0.4	-0.9	0.6	-0.7	-1.2	-1.4	-1.4	-1.3	-1.2	-0.1	-0.2	-0.6	0.1	0.7	0.8	0.5	-1.1
80.	0.3	-0.7	0.5	0.3	-0.7	-1.1	-1.0	-0.8	0.0	-0.6	-0.3	0.0	0.5	0.7	1.0	0.6	-0.5
70.	0.2	0.2	0.1	-0.1	0.0	-0.2	-0.6	-0.3	0.1	-0.3	0.0	0.4	0.4	0.9	1.2	0.7	-0.2
60.	0.1	0.8	0.4	0.7	0.0	-0.4	0.0	-0.1	-0.3	0.0	0.2	0.1	0.7	0.9	1.1	0.7	0.0
50.	0.9	1.0	0.0	-0.1	0.0	0.0	0.0	0.0	-0.3	0.1	0.1	0.3	0.5	1.0	1.1	0.8	0.4
40.	0.4	0.1	0.3	-0.2	0.0	-0.2	-0.2	-0.2	0.0	0.0	0.0	0.1	0.3	0.7	1.1	0.7	0.4
30.	-0.3	-0.1	0.0	0.0	0.0	-0.1	0.0	-0.3	-0.2	-0.2	0.0	0.0	0.3	0.5	0.7	0.5	0.4
20.	-0.3	-0.4	-0.4	-0.2	-0.4	-0.6	-0.5	-0.4	-0.5	-0.3	-0.3	-0.1	0.0	0.1	0.2	0.3	0.2
10.	-0.5	-0.5	-0.5	-0.7	-0.8	-0.8	-0.7	-0.9	-0.8	-1.0	-0.8	-0.8	-0.5	-0.3	-0.3	-0.5	-0.5

PERCENT ERROR ON GAMMA

VEL	-40.	-35.	-30.	-25.	-20.	-15.	-10.	-5.	0.	5.	10.	15.	20.	25.	30.	35.	40.
120.	2.3	-4.3	-4.9	-3.3	2.3	7.6	11.8	11.8		11.8	11.8	7.6	2.3	-0.7	-4.9	-4.3	0.7
110.	2.3	-4.3	-4.9	-3.3	2.3	3.4	11.8	11.8		11.8	5.5	7.6	2.3	-3.3	-4.9	-4.3	0.7
100.	0.7	-4.3	-4.9	-3.3	-0.7	7.6	11.8	11.8		11.8	5.5	3.4	2.3	-3.3	-4.9	-4.3	0.7
90.	0.7	-4.3	-7.0	-3.3	2.3	7.6	11.8	24.4		11.8	11.8	3.4	2.3	-0.7	-2.8	-2.5	0.7
80.	0.7	-4.3	-7.0	-5.8	2.3	7.6	11.8	11.8		-0.7	5.5	7.6	2.3	-3.3	-4.9	-4.3	0.7
70.	0.7	-4.3	-7.0	-3.3	-0.7	3.4	11.8	11.8		11.8	5.5	7.6	2.3	-0.7	-4.9	-4.3	0.7
60.	0.7	-6.1	-7.0	-5.8	-0.7	7.6	5.5	11.8		-0.7	5.5	3.4	2.3	-3.3	-4.9	-4.3	0.7
50.	0.7	-6.1	-7.0	-3.3	-0.7	3.4	5.5	11.8		-0.7	5.5	7.6	-0.7	-0.7	-4.9	-4.3	2.3
40.	0.7	-6.1	-9.1	-3.3	-0.7	3.4	11.8	11.8		11.8	5.5	3.4	-0.7	-3.3	-0.7	-2.5	3.9
30.	0.7	-4.3	-7.0	-5.8	-3.9	3.4	5.5	18.8		-0.7	5.5	3.4	-3.3	-3.3	-2.8	-2.5	5.5
20.	2.3	-2.5	-7.0	-8.3	5.5	3.4	5.5	-0.7		11.8	-0.7	3.4	2.3	-0.7	1.3	2.8	10.2
10.	5.5	-2.5	-7.0	-5.8	-7.0	-0.7	5.5	49.6		-0.7	5.5	3.4	-0.7	-0.7	-2.8	4.6	13.3

DIFFERENCE ON GAMMA (DEG)

VEL	-40.	-35.	-30.	-25.	-20.	-15.	-10.	-5.	0.	5.	10.	15.	20.	25.	30.	35.	40.
120.	0.9	-1.5	-1.4	-0.8	0.4	1.1	1.1	0.5	0.0	-0.5	-1.1	-1.1	-0.4	0.1	1.4	1.5	-0.3
110.	0.9	-1.5	-1.4	-0.8	0.4	0.5	1.1	0.5	0.6	-0.5	-0.5	-1.1	-0.4	0.8	1.4	1.5	-0.3
100.	0.3	-1.5	-1.4	-0.8	-0.1	1.1	1.1	0.5	0.6	-0.5	-0.5	-0.5	-0.4	0.8	1.4	1.5	-0.3
90.	0.3	-1.5	-2.1	-0.8	0.4	1.1	1.1	1.2	0.6	-0.5	-1.1	-0.5	-0.4	0.1	0.8	0.9	-0.3
80.	0.3	-1.5	-2.1	-1.4	0.4	1.1	1.1	0.5	0.0	0.0	-0.5	-1.1	-0.4	0.8	1.4	1.5	-0.3
70.	0.3	-1.5	-2.1	-0.8	-0.1	0.5	1.1	0.5	0.0	-0.5	-0.5	-1.1	-0.4	0.1	1.4	1.5	-0.3
60.	0.3	-2.1	-2.1	-1.4	-0.1	1.1	0.5	0.5	0.6	0.0	-0.5	-0.5	-0.4	0.8	1.4	1.5	-0.3
50.	0.3	-2.1	-2.1	-0.8	-0.1	0.5	0.5	0.5	0.6	0.0	-0.5	-1.1	0.1	0.1	1.4	1.5	-0.9
40.	0.3	-2.1	-2.7	-0.8	-0.1	0.5	1.1	0.5	0.6	-0.5	-0.5	-0.5	0.1	0.8	0.2	0.9	-1.5
30.	0.3	-1.5	-2.1	-1.4	-0.7	0.5	0.5	0.5	0.6	0.0	-0.5	-0.5	0.1	0.8	0.8	0.9	-2.2
20.	0.9	-0.9	-2.1	-2.0	1.1	0.5	0.5	0.0	0.6	-0.5	0.0	-0.5	-0.4	0.1	-0.3	-0.9	-4.0
10.	2.2	-0.9	-2.1	-1.4	-1.4	-0.1	0.5	2.4	1.2	0.0	-0.5	-0.5	0.1	0.1	0.8	-1.6	-5.3

Table 3. Ability of interpolation formulae to reproduce calibration data.
Note: Data columns represent γ values over the range: $-40^\circ \leq \gamma \leq 40^\circ$.